Project Title: An Integrated Approach to Characterizing Bypassed Oil in Heterogeneous and Fractured Reservoirs Using Partitioning Tracers

ANNUAL REPORT
Reporting Period Start Date: June 2004
Reporting Period End Date: June 2005

Principal Author: Akhil Datta-Gupta
August, 2005

DOE Contract No. DE-FC26-02NT15345

Submitting Organization:
Texas Engineering Experiment Station
Texas A&M University, College Station, TX

Subcontractor: Gary A. Pope
Petroleum and Geosystems Engineering
University of Texas, Austin, TX

DISCLAIMER

ABSTRACT

We explore the use of efficient streamline-based simulation approaches for modeling and analysis partitioning interwell tracer tests in heterogeneous and fractured hydrocarbon reservoirs. We compare the streamline-based history matching techniques developed during the first two years of the project with the industry standard assisted history matching. We enhance the widely used assisted history matching in two important aspects that can significantly improve its efficiency and effectiveness. First, we utilize streamline-derived analytic sensitivities to relate the changes in reservoir properties to the production response. These sensitivities can be computed analytically and contain much more information than that used in the assisted history matching. Second, we utilize the sensitivities in an optimization procedure to determine the spatial distribution and magnitude of the changes in reservoir parameters needed to improve the history-match. By intervening at each iteration during the optimization process, we can retain control over the history matching process as in assisted history matching. This allows us to accept, reject, or modify changes during the automatic history matching process. We demonstrate the power of our method using two field examples with model sizes ranging from 10^5 to 10^6 grid blocks and with over one hundred wells. We have also extened the streamline-based production data integration technique to naturally fractured reservoirs using the dual porosity approach. The principal features of our method are the extension of streamline-derived analytic sensitivities to account for matrix-fracture interactions and the use of our previously proposed generalized travel time inversion for history matching. Our proposed workflow has been demonstrated by using both a dual porosity streamline simulator and a commercial finite difference simulator. Our approach is computationally efficient and well suited for large scale field applications in naturally fractured reservoirs with changing field conditions. This considerably broadens the applicability of the streamline-based analysis of tracer data and field production history for characterization of heterogeneous and fractured reservoirs.

TABLE OF CONTENTS

EXECUTIVE SUMMARY

During the third year of the project, we compared the streamline-based history matching techniques developed during the first two years of the project with the industry standard assisted history matching. We enhance the widely used assisted history matching in two important aspects that can significantly improve its efficiency and effectiveness. First, we utilize streamline-derived analytic sensitivities to relate the changes in reservoir properties to the production response. These sensitivities can be computed analytically and contain much more information than that used in the assisted history matching. Second, we utilize the sensitivities in an optimization procedure to determine the spatial distribution and magnitude of the changes in reservoir parameters needed to improve the history-match. By intervening at each iteration during the optimization process, we can retain control over the history matching process as in assisted history matching. This allows us to accept, reject, or modify changes during the automatic history matching process. We demonstrate the power of our method using two field examples with model sizes ranging from 10^5 to 10^6 grid blocks and with over one hundred wells. The reservoir models include faults, aquifer support and several horizontal/high angle wells. History matching was performed using both assisted history matching and our previously proposed generalized travel time inversion, (GTTI). Whereas the general trends in permeability changes were similar for both the methods, the GTTI seemed to significantly improve the water cut history matching on a well-by-well basis within a few iterations. Our experience indicates that the GTTI can also be used very effectively to improve the quality of history match derived from the assisted history matching. The changes to the reservoir model from GTTI were found reasonable with no artificial discontinuities or apparent loss of geologic realism. Most importantly, history matching using GTTI took only few hours as compared to weeks or months by assisted history matching.

We have also extened the streamline-based production data integration technique to naturally fractured reservoirs using the dual porosity approach. The principal features of our method are the extension of streamline-derived analytic sensitivities to account for matrix-fracture interactions and the use of our previously proposed generalized travel time inversion for history matching. Our proposed workflow has been demonstrated by using both a dual porosity streamline simulator and a commercial finite difference simulator. Our approach is computationally efficient and well suited for large scale field applications in naturally fractured reservoirs with changing field conditions. The use of the generalized travel time concept enabled us to match both the breakthrough and amplitude of the reference response in one step.

This report is divided into two major parts. The first part describes the comparison between industry standard assisted history matching and our proposed streamline-based generalized travel time inversion. Two large field examples are presented to demonstrate the power and utility of our method compared to the current industry practice. The second part of the report generalizes our approach to naturally fractured reservoirs using the dual porosity streamline simulation. This considerably broadens the applicability of the streamline-based analysis of tracer data and field production history for characterization of heterogeneous and fractured reservoirs.

The following papers were published based on the work from the third year of this research project.

- Cheng, H., Wen, X, Milliken, W. and Datta-Gupta, A., "Field Experiences with Assisted and Automatic History Matching Using Streamline Models," SPE 89857 presented at the SPE Annual Technical Conference and Exhibition, Houston, TX, September 26-29, 2004.

- Al-Harbi, M., Cheng, H., He, Zhong and Datta-Gupta, A., "Streamline-based Production Data Integration in Naturally Fractured Reservoirs," presented at the SPE Annual Technical Conference and Exhibition, Houston, TX, September 26-29, 2004. Accepted for publication in *SPE Journal* (2005)

INTRODUCTION

Reconciling high-resolution geologic models to production history is a very time-consuming aspect in reservoir modeling. Current industry practice still involves a tedious history-matching process that is highly subjective and often employs ad-hoc property multipliers. Recently streamline models have shown significant promise in improving the efficiency of history matching process. In particular, the streamline-based 'assisted history-matching' utilizes the streamline trajectories to identify and limit changes only to the regions contributing to the well production history. It is now a well-established procedure and has been applied successfully to numerous field cases. Over the past two years, we have developed a systematic procedure for history matching high resolution geologic models using streamline-based analytic sensitivities. In this phase of the work, we compare our approach with the industry standard 'assisted' history matching and also generalize its applicability to fractured systems.

Field Experiences with Assisted and Automatic History Matching Using Streamline Models

In this work, we enhance the streamline-based assisted history matching in two important aspects that can significantly improve its efficiency and effectiveness. First, we utilize streamline-derived analytic sensitivities to determine the spatial distribution and magnitude of the changes needed to improve the history match. Second, we use a 'generalized travel time inversion (GTTI)' for model updating via an iterative minimization procedure. Using this approach, we can account for the full coupling of the streamlines rather than changing individual or bundles of streamlines at a time. The approach is more akin to automatic history matching; however, by intervening at every step in the iterative model updating, we can retain control over the process as in assisted history matching. Our approach leads to significant savings in time and manpower during field-scale history matching.

We demonstrate the power of our method using two field examples with model sizes ranging from 10^5 to 10^6 grid blocks and with over one hundred wells. The reservoir models include faults, aquifer support and several horizontal/high angle wells. History matching was performed using both assisted history matching and the GTTI. Whereas the general trends in permeability changes were similar for both the methods, the GTTI seemed to significantly improve the water cut history matching on a well-by-well basis within a few iterations. Our experience indicates that the GTTI can also be used very effectively to improve the quality of history match derived from the assisted history matching. The changes to the reservoir model from GTTI were found reasonable with no artificial discontinuities or apparent loss of geologic realism.

Streamline-Based Production Data Integration in Naturally Fractured Reservoirs

Streamline-based models have shown great potential in reconciling high resolution geologic models to production data. In this work we extend the streamline-based production data integration technique to naturally fractured reservoirs. Describing fluid transport in fractured reservoirs poses additional challenge arising from the matrix-fracture interactions. We use a dual-porosity streamline model for fracture flow simulation by treating the fracture and matrix as separate continua that are connected through a transfer function. Next, we analytically compute

the sensitivities that define the relationship between the reservoir properties and the production response in fractured reservoirs. The sensitivities are an integral part of our approach and can be evaluated very efficiently as 1-D integrals along streamlines. Finally, the production data integration is carried out via a generalized travel time inversion which has been shown to be robust because of its quasi-linear properties and utilizes established techniques from geophysical inverse theory.

We also apply the streamline-derived sensitivities in conjunction with a dual porosity finite difference simulator to combine the efficiency of the streamline approach with the versatility of the finite difference approach. This significantly broadens the applicability of the streamline-based approach in terms of incorporating compressibility effects and complex physics. We demonstrate the power and utility of our approach using 2-D and 3-D synthetic examples designed after actual field conditions. The reference fracture patterns are generated using a discrete fracture network (DFN) model that allows us to include statistical properties of fracture swarms, fracture densities and network geometries. The DFN is then converted to a continuum model with equivalent grid block permeabilities. Starting with prior models with varying degrees of fracture information, we match the water-cut history from the reference model. Both dual porosity streamline and finite difference simulators are used to model fluid flow in the fractured media. Our results indicate the effectiveness of our approach and the role of prior information and production data in reproducing fracture connectivities and preferential flow paths.

EXPERIMENTAL

No experiments were performed during the second year of the project.

RESULTS AND DISCUSSION: PART I

Field Experiences with Assisted and Automatic History Matching Using Streamline Models

Introduction

Geostatistical reservoir models are widely used to model the heterogeneity of reservoir petrophysical properties, such as permeability and porosity. These geostatistical reservoir models are usually upscaled from fine-scale geologic/geocellular models to coarser reservoir simulation models for field development studies and performance predictions.

It is imperative that geostatistical reservoir models incorporate as much available, site-specific information as possible in order to reduce the uncertainty in the subsurface characterization. Available information on reservoir heterogeneity can be broadly categorized into two major types: static and dynamic. Static data are time-invariant direct or indirect measurements of reservoir properties, such as core measurements, well logs, and seismic data. These data can, relatively easily, be integrated into geostatistical models using the traditional geostatistical algorithms.[1] Dynamic data are the time dependent measurements of flow responses that are related to the reservoir properties through the flow equations, such as pressure, flow rate, fractional flow rate, or saturation. Integration of dynamic data generally leads to an inverse problem and requires the solution of the flow equations several times using an iterative procedure.[2-3] The process is generally referred to as "history matching" and is usually the most tedious and time-consuming aspect of a reservoir simulation study.

Traditionally, history matching is performed manually on the upscaled reservoir model and frequently uses local or regional multipliers to reservoir properties. By adjusting the regions and multipliers, a history match could be achieved using mostly trial and error. The trial-and-error involves considerable subjective judgment and personal bias and most importantly may create artificial discontinuities inside the reservoir, potentially destroying the correlation built into the initial geologic model.

A more systematic approach to history matching, called Assisted History Matching (AHM) uses streamlines to build upon and improve traditional history matching techniques.[4-6] The AHM is also a manual approach. However, changes to the model can be limited to the streamlines contributing to the production history of the well of interest and the amount of changes can be computed using some simple semi-analytical methods. The approach is a significant improvement over the traditional manual history matching but still could be time consuming, particularly when there are a large number of wells. This is complicated by the coupled nature of the flow equations which makes matching individual wells difficult without impacting other wells also. Finally, if we limit changes along streamlines only, it can introduce 'tube like' artifacts into the geologic model.

Geostatistically-based automatic history matching (production data integration) has been an active area of research and a number of techniques have been reported in the literature in the past decade. The main goal here is to match well production data by modifying the initial model in such a way that it preserves the underlying geostatistical features built into the initial model. Yeh[7] and Wen *et al.*[8] provided a review of these inverse techniques. Both finite difference and

streamline fluid flow modeling can be used in automated history matching.[9] Typically, an inverse technique is needed for production data integration, and requires multiple solutions of the flow equations within a nonlinear optimization procedure.[10-12] And this brings a hurdle to the practical applications. Streamline based inverse techniques have shown great potential in this regard[13-18] and they only require a single solution of the flow equations per minimization iteration.[13-14] The sensitivities of production data with respect to reservoir properties can be computed analytically using a single forward simulation. This renders substantial time-saving.

Much of the ideas of AHM are actually embedded in the streamline-based sensitivity computations. The sensitivities define the relationship between reservoir properties and production response. Specifically, they quantify how, for example, the water-cut history at a well will change if we change permeability at any location in the reservoir model. Using the sensitivities, we can significantly speed-up the assisted history matching process and compute the amount of changes for reservoir properties through optimization. Instead of matching wells individually, we can handle the coupled problem directly and update the geologic model to match all the wells simultaneously. The approach is more akin to automatic history matching; however, by intervening at every step in the iterative model updating, we can retain control over the process as in assisted history matching.

In this work we enhance the streamline-based assisted history matching in two important aspects that can significantly improve its efficiency and effectiveness. First, we utilize streamline-derived analytic sensitivities to determine the spatial distribution and magnitude of the changes needed to improve the history-match. These sensitivities are then incorporated into an optimization algorithm to update the reservoir model during flow simulation. Secondly, a "generalized travel-time inversion (GTTI)"[19-20] is used for inverse modeling. The GTTI is robust because of its quasi-linear properties[21] resulting in rapid convergence even if the prior model is far from the solution. We demonstrate our approach using two field examples with over 100 wells and more than 30 years of production history.

Background and Illustrative Examples

Assisted History Matching. Assisted history matching utilizes unique information-content in streamlines in terms of injector-producer relationship to facilitate history matching.[4-5] The main steps in assisted history matching are: (i) Flow simulation to generate production response. Either streamline or finite-difference simulators can be used for this purpose; (ii) Streamline generation based on the finite-difference velocity field. This step is not necessary for streamline simulators as streamlines are already available; (iii) Use of streamlines to assign grid blocks or regions to each producer; (iv) Computing the mismatch between the observed and computed production response at each well using streamlines; (v) Updating grid block or region properties manually to improve the history match on a well-by-well basis. The use of streamlines leads to simple and unambiguous changes in the model. Also, the changes are minimized to preserve the geology. An outline of the procedure of assisted history matching is given in a flow chart in **Fig. 1**.

Illustration of the Procedure. **Fig. 2** shows a 2D reference permeability field (50×50 grid with cell size 10 feet × 10 feet) generated using Sequential Gaussian Simulation[1] and the corresponding fractional-flow data at four producing wells in 5-spot pattern. The variogram of the reference field is spherical with range of 100 feet and 20 feet in the direction of 45 degree and 135 degree, respectively. We generated an initial model using the same geostatistical method with the same histogram and variogram as for the reference field. The initial permeability and the

water cut responses from the four corner wells are shown in **Fig. 3**. Note that this initial model visually is quite close to the reference model. The flow responses, however, are quite different from the reference model. **Fig. 4** shows the streamlines for the initial model. Now in order to match the reference water cut, streamlines are used to help assigning cells to wells and grouping the cells. From streamlines, we know which cells to change to history match a particular well. Besides, we know which streamlines contribute to early breakthrough (A), middle stage (B), and later stage (C) water cut. Streamline helps grouping cells that need to be modified. We can change cells covered by streamlines marked 'A' to match early breakthrough, and change those associated with 'B' and 'C' to match middle and later stage water cut.

The assisted history matching can accelerate the history matching process significantly. However, the approach is still more or less manual and requires some trial and error. Individual well matching can sometimes deteriorate matches in other wells because of the coupled nature of the flow field. Finally, limiting the changes to streamlines can introduce artifacts in the geologic model unless the changes are kept to a minimum. Recently, a number of approaches have been reported to improve the efficiency of the AHM method. These include the use of tracer-like flow assumption to compute the modifications of reservoir properties within the well regions delineated by streamlines that can match multiple phase production history,[17,22] and the integration of streamline information at different levels with geostatistics.[16,23] These approaches, however, do not directly use the sensitivity coefficients derived from the streamline simulation to quantify the changes. Therefore, the improvement in efficiency is marginal at best.

Streamline-Based Automatic History Matching. This approach utilizes streamline-derived sensitivities to update geologic models.[9,13,14,20] The major steps are: (i) Streamline-based flow simulation to compute production response at the wells; (ii) Quantification of the mismatch between observed and computed production response; (iii) Streamline-based analytic sensitivity computation of the production response with respect to reservoir parameters; (iv) Updating reservoir properties to match the production history via inverse modeling using streamline-derived sensitivities. An outline of the procedure of streamline-based automatic history matching is given in a flow chart in **Fig. 5**.

Illustration of the Procedure. To illustrate the procedure, we use the same synthetic example used for assisted history matching. We have used a commercial 3D streamline simulator, FrontSim[33] (Version 2003a), for modeling two-phase flow in the reservoir. Production data misfit is represented by a 'generalized travel time' at each producing well. A "generalized travel time" or "travel-time shift" is computed by systematically shifting the computed production response towards the observed data until the cross-correlation between the two curves is maximized.[19-20] This is illustrated in **Fig. 6** and is discussed further later. The sensitivities calculated for automatic history matching are shown in **Fig. 7**. These sensitivities are calculated along the streamlines analytically using time of flight and fractional flow information. Unlike assisted history matching, there is no need for manual intervention to look at the streamlines to determine where to change the models. Also, with the sensitivity information, we can apply different modifications determined from optimization to different locations. **Figs. 7d** and **7e** show that sensitivities are calculated along the streamlines. The largest sensitivities in magnitude (dark-blue region) correspond to early breakthrough, and the medium (light-blue to green) and small (yellow) sensitivities correspond to middle stage and later stage water cut. Also the whole region covered by the sensitivities will be changed systematically and automatically by generalized travel-time inversion. **Fig. 8** shows that the water-cut responses are in good

agreement with the reference, and the updated permeability model maintains the general features of the initial model. As desired, the permeability was increased around Well 2 while decreased around Well 3 to match the history (**Fig. 9**, also refer to Fig. 3 for the initial model). The decrease of objective function (shift time) with the iteration number, as well as the associated water-cut misfit, is shown in **Fig. 10**. The shift time objective function reduces from 670 days to 20 days in 20 iterations, and it reduces quickly in the first few iterations.

Multiple realizations. An important advantage of the streamline-based inversion is its computational efficiency. This makes dynamic conditioning of multimillion-cell models feasible using the streamline approach. In addition, we are able to generate multiple realizations to assess uncertainty in performance forecasting, for example, using the randomized maximum likelihood method.[24] Using multiple realizations and an ensemble average map, we can also reveal large-scale spatial trends common to all realizations. To illustrate this, we generated 100 initial models and history matched all of them to the reference production data in 4 wells using the streamline-based inversion. Initial realizations are generated by unconditional Gaussian simulation with the same histogram and variogram as for the reference field.

The water-cut responses from all initial and updated realizations are shown in **Figs. 11** and **12**. Clearly, after inversion, the calculated water-cut responses all moved much closer to the reference responses (Fig. 12). Note that in the randomized maximum likelihood method we match "realizations" of the observed production history rather than the history itself; hence, we see the spread in the water-cut responses in the updated models. For 100 realizations, it took only 150 minutes in a PC (Intel Xeon 3.06 GHz processor). The mean and variance of the 100 realizations is shown in **Fig. 13**. The final ensemble mean field captured most of the low permeability region and some of the high permeability region (**Fig. 13a**), while the variance field (**Fig. 13b**) displays the uncertainty among the updated models.

Streamline-Based Automatic History Matching: Mathematical Formulation

Several previous publications describe streamline-based sensitivity computations and generalized travel time inversion.[9,13-14,18-20] In this section, we briefly outline the mathematical background behind the approach.

Forward Modeling: Streamline Simulation. Streamline simulators approximate 3D fluid flow calculations by a sum of 1D calculations along streamlines. The choice of streamline direction for 1D calculations makes the approach extremely effective for modeling convection-dominated flows in the reservoir.[27] This is typically the case when heterogeneity is the predominant factor controlling oil recovery, for example in waterflooding. The streamline approach for modeling multidimensional, multiphase flow basically comprises of five major steps:[26-29] (i) Tracing streamlines in 3D based on a numerical solution of the pressure and velocity equations; (ii) Recasting the transport (saturation) equations in terms of streamline time of flight which is the travel time of a tracer along the streamline; (iii) Solution of the saturation equation along streamlines; (iv) Periodic updating of streamlines to account for changing field conditions such as infill drilling and rate changes; (v) Use of operator splitting to account for transverse fluxes such as gravity.

The computational advantage of the streamline methods can be attributed to four principal reasons: (i) Streamlines may need to be updated only infrequently; (ii) The transport equations along streamlines can often be solved analytically; (iii) The 1D numerical solutions along streamlines are not constrained by the underlying grid stability criteria, thus allowing for larger

timesteps; (iv) For displacements dominated by heterogeneity, the CPU time often scales nearly linearly with the number of gridblocks, making it the preferred method for fine-scale geologic simulations. Furthermore, the self-similarity of the solution along streamlines may allow us to compute the solution only once and map it to the time of interest. Other advantages are sub-grid resolution and reduced numerical artifacts such as artificial diffusion and grid orientation effects, since the streamline grid used to solve the transport equations is effectively decoupled from the underlying static grid.

Generalized Travel Time and Sensitivity Calculations. As shown in **Fig. 6**, we define the generalized travel time as the optimal time shift $\Delta\tilde{t}$ that maximizes the following correlation function:

$$R^2(\Delta t_j) = 1 - \frac{\sum\left[y_j^{obs}(t_i+\Delta t_j) - y_j^{cal}(t_i)\right]^2}{\sum\left[y_j^{obs}(t_i) - \overline{y_j^{obs}}\right]^2}, \quad \text{..... (1)}$$

where y is the flow responses we wish to match, e.g., water cut at producing wells, j is producer index and i is observation data index. The overall production data misfit can now be expressed in terms of a generalized travel-time misfit at all wells as $\sum_{j=1}^{N_w}(\Delta\tilde{t}_j)^2$, with N_w being the total number of producing wells. Our objective is to minimize this generalized travel time misfit, and we need the sensitivities for minimization.

Sensitivity Computations. In GTTI, we shift the entire fractional flow curve by a constant time. Thus, every data point in the fractional-flow curve has the same shift time, $\delta t_1 = \delta t_2 = \cdots = \Delta\tilde{t}$ (Fig. 6). So we can sum up and average the travel time sensitivities of all data points to obtain a rather simple expression for the sensitivity of the generalized travel time with respect to reservoir parameters m as follows[20]

$$\frac{\partial \Delta\tilde{t}_j}{\partial m} = -\frac{\sum_{i=1}^{N_{dj}}\left(\partial t_{i,j}/\partial m\right)}{N_{dj}}. \quad \text{.....(2)}$$

It now reduces to the sensitivity of the arrival times at the producing well, $\partial t_{i,j}/\partial m$. These sensitivities can be easily obtained in terms of the sensitivities of the streamline time of flight,[20]

$$\frac{\partial t}{\partial m} = \frac{\dfrac{\partial \tau}{\partial m}}{\dfrac{\partial f_w}{\partial S_w}}. \quad \text{.....(3)}$$

In the above expression, the fractional-flow derivatives are computed at the saturation of the outlet node of the streamline. The time-of-flight sensitivities can be obtained analytically in terms of simple integrals along streamline. For example, the time-of-flight sensitivity with respect to permeability will be given by[13]

$$\frac{\partial \tau}{\partial k(\mathbf{x})} = \int_{\Sigma}\frac{\partial s(\mathbf{x})}{\partial k(\mathbf{x})}dx = -\int_{\Sigma}\frac{s(\mathbf{x})}{k(\mathbf{x})}dx, \quad \text{.....(4)}$$

where the integrals are evaluated along the streamline trajectory, and the 'slowness' which is the reciprocal of interstitial velocity, is given by

$$s(\mathbf{x}) = \frac{\phi(\mathbf{x})}{\lambda_t k(\mathbf{x})|\nabla P(\mathbf{x})|} \quad \text{.....(5)}$$

Note that the quantities in the sensitivity expressions are either contained in the initial reservoir model or are available after the forward simulation run.

Data Integration. Our goal is to reconcile high-resolution geologic models to field production history. This typically involves the solution of an underdetermined inverse problem. The mathematical formulation behind such streamline-based inverse problems has been discussed elsewhere.[13,28] Both the deterministic and stochastic approaches have been used with equal success.[30] In the deterministic approach pursued here, we start with a prior static model that already incorporates geologic, well log, and seismic data. We then minimize a penalized misfit function consisting of the following three terms,

$$\left\|\Delta\tilde{\boldsymbol{t}} - \boldsymbol{G}\delta\boldsymbol{m}\right\| + \beta_1\left\|\delta\boldsymbol{m}\right\| + \beta_2\left\|\boldsymbol{L}\delta\boldsymbol{m}\right\| \quad \text{.....(6)}$$

In **Eq. 6**, $\Delta\tilde{\boldsymbol{t}}$ is the vector of generalized travel-time shift at the wells; $\boldsymbol{G}$ is the sensitivity matrix containing the sensitivities of the generalized travel time with respect to the reservoir parameters. Also, $\delta\boldsymbol{m}$ correspond to the change in the reservoir property and $\boldsymbol{L}$ is a second spatial difference operator that is a measure of roughness and is analogous to imposing a prior variogram or covariance constraint. The first term ensures that the difference between the observed and calculated production response is minimized. The second term, called a 'norm constraint', penalizes deviations from the initial model. This helps preserve geologic realism because our initial or prior model already incorporates available geologic and static information related to the reservoir. Finally, the third term, a roughness penalty, simply recognizes the fact that production data are an integrated response and are thus, best suited to resolve large-scale structures rather than small-scale property variations. The minimum in Eq. 6 can be obtained by an iterative least-squares solution to the augmented linear system

$$\begin{pmatrix} \boldsymbol{G} \\ \beta_1\boldsymbol{I} \\ \beta_2\boldsymbol{L} \end{pmatrix}\delta\boldsymbol{m} = \begin{pmatrix} \Delta\tilde{\boldsymbol{t}} \\ \boldsymbol{0} \\ \boldsymbol{0} \end{pmatrix} \quad \text{.....(7)}$$

The weights β_1 and β_2 determine the relative strengths of the prior model and the roughness term. In general, the inversion results will be sensitive to the choice of these weights.

When the data and the prior model statistics are specified, for example, the data errors and model parameter covariance (variogram), we can adopt a Bayesian formulation that leads to the minimization of the following function,

$$\frac{1}{2}\left(m - m_p\right)^T C_M^{-1}\left(m - m_p\right) + \frac{1}{2}\left[\Delta\tilde{\boldsymbol{t}}\right]^T C_D^{-1}\left[\Delta\tilde{\boldsymbol{t}}\right] \quad \text{.....(8)}$$

The minimum in **Eq. 8** can be obtained by an iterative least-squares solution to the linear system[30]

$$\begin{bmatrix} \boldsymbol{C}_D^{-1/2}\boldsymbol{G} \\ \boldsymbol{C}_M^{-1/2} \end{bmatrix}\delta\boldsymbol{m} = \begin{bmatrix} \boldsymbol{C}_D^{-1/2}\left(\Delta\tilde{\boldsymbol{t}}\right) \\ \boldsymbol{C}_M^{-1/2}\left(\boldsymbol{m}_p - \boldsymbol{m}\right) \end{bmatrix} \quad \text{.....(9)}$$

where $\boldsymbol{C_D}$ and $\boldsymbol{C_M}$ are the data error covariance and the prior model parameter covariance respectively, and $\boldsymbol{m}_p$ is the prior term. **Eq. 9** represents a system of equations that is analogous to the deterministic formulation in **Eq. 7**. We use an iterative sparse matrix solver, LSQR, for solving these augmented linear systems in Eqs. 7 and 9. The LSQR algorithm is well suited for

highly ill-conditioned systems and has been widely used for large-scale tomographic problems in seismology.[31]

It is important to realize that automatic history matching does not necessarily imply that the user has to lose control over the process. Instead, it is recommended that the user intervene after every iteration of the process to determine the plausibility of the changes and accept or reject or modify the changes. From this point of view, the only difference from assisted history matching is the use of the sensitivities and the non-linear optimization technique to determine the spatial location and the extent of changes to the prior model.

Field Examples

We now discuss applications of streamline-based assisted and automatic history matching to two field examples. We illustrate the use of automatic history matching both for conditioning static geologic models to production data and also as a "finisher/post-processor" to assisted history matching to further improve the matches.

Field Example 1. The first model we studied is a cutout section from a large sandstone reservoir containing over 1.5 MMMSTB of oil.[5] The reservoir is characterized by three principal depositional settings, incised channel fill, regional marine shale, and tidal delta complex. The sector we considered has an average porosity of 20% (**Fig. 14**) with median permeability of about 1000 md. The grid dimensions are 30×46×39 (53,820 cells). The model has two faults, an aquifer, and four different relative permeability zones. The oil is a 36º API gravity oil with a viscosity of 0.3 cp at reservoir conditions. The field has been produced for approximately 50 years by primary depletion and phased waterflooding. The simulation model starts at Year 1965 and ends at Year 2001. Recovery to Year 2001 is approximately 35% OOIP with a field-wide water cut of approximately 93%. Altogether there are 130 wells in the simulation and history matching process. Only water-cut history was used to update the permeability model.

For automatic history matching, we will use two different starting models. In the first case, the initial model is up-scaled directly from the static fine-scale geostatistical model using flow-based upscaling method. [32] This initial model was used in both assisted and automatic history matching. In the second case, the initial model is the updated permeability model after assisted history matching.[5] Our goal in this second case is to use automatic history matching to further improve the results of assisted history matching.

We choose horizontal permeability as our model parameter in the inversion. Vertical permeability is also changed during the inversion by preserving the ratio of horizontal and vertical permeability. Porosity in the model was not altered because its variation was relatively minor compared to permeability.

Assisted vs. Automatic History Matching. **Fig. 15** shows the field-wide water-cut performance for the initial geologic model, the updated model by automatic history matching, as well as the result from assisted history matching. We can see that the initial model shows large deviations from the field production history. The results from automatic history matching exhibit significant improvement in the water-cut match. For this case, the matches from the automatic history matching appear to be better than that of assisted history matching, particularly in the early period.

The water-cut match for a few typical wells from amongst the 130 wells is given in **Fig. 16**. For validation purposes, we matched only part of the history data for some wells and used the updated model to predict the production performance for the rest of the period. For example, for

Well 128 we matched the data only to Year 1989. Clearly, the prediction for the rest of time period shows marked improvement compared to the initial model. The permeability models before and after automatic history matching are shown in **Fig. 17**. The inverted model has increased heterogeneity by increasing the permeability contrast and variance. In some areas, the permeabilities are increased and in other areas decreased. Overall, the final updated model by automatic history matching preserved most of the prior geologic features while improving the history match.

It should be noted that production data smoothing is an important step during generalized travel-time inversion with field data. The field production history data are frequently erratic with numerous fluctuations. Very often, the time step sizes used in the streamline simulation are larger than the intervals of observed data. Thus, the short-term fluctuations in the production data are not captured by simulation. We averaged the production data before inversion over pre-specified interval using the simulation time steps as guidelines. This helps the inversion to capture the general trend of the production history and not to be trapped by small details. Data smoothing also facilitates the calculation of the shift time during generalized travel-time calculations.

As mentioned before, the automatic history matching using streamline-derived sensitivities is very computationally efficient. For this case, it took about 5 hours for IBM Regatta workstation for 8 inversion iterations and less than one week, including the setup time, for the entire history match. Assisted history matching for the same field case will generally take much longer, of the order of a few months depending upon the experience level of the user.

Automatic History Matching as 'Post Processor' to Assisted History Matching. Here we utilize automatic history matching to further improve upon the geologic model derived from assisted history matching. The field-wide water-cut match after assisted history matching is already quite close to the history data (**Fig. 18**). After automatic history matching, it is further improved, particularly in the early time (see the enlarged figure of early time section on the right of Fig. 18).

For individual well-by-well water-cut matches, most wells show further significant improvement over assisted history matching (see **Fig. 19** for some typical wells from 130 wells). For example, the water cuts in some wells (e.g., Wells 50, 67) are shifted right to match the history, while some are shifted left (e.g., Wells 12, 89, 99) to match the history. The most significant improvement is observed for Well 99. For very few wells (3 wells), the water cut in the updated model is slightly worse than the initial model. After eight iterations, the objective function was reduced by half, and the water-cut misfit was reduced by 20 to 30 percent. Each inversion iteration consists of one forward (FrontSim[33]) simulation (about 30 minutes) and one LSQR solution (about 8 minutes). The entire history match process took about 5 hours for eight iterations in IBM Regatta workstation

Fig. 20 shows the permeability models before and after automatic history matching. From a visual inspection we see that most of the features in the initial model are preserved in the updated model. However, comparing on a layer-by-layer basis, we can find some detailed changes in the model. We show a number of layers where the main changes occur. **Fig. 21** shows the permeability histogram for four different cases: (i) the initial static geologic model, (ii) the updated model via automatic history matching starting from the initial geologic model, (iii) the updated model via assisted history matching starting from the initial geologic model, and (iv) the updated model via automatic history matching starting from assisted history-matched model. We can see that the automatic history matching leads to a similar permeability statistics regardless of

whether we started from the initial model or the updated model after assisted history matching. We can see that the low permeability at the initial geological model have been removed, indicating the need to increase permeability at the low permeability regions to match the production data. Interestingly, the histograms of the permeability models from assisted history matching and automatic history matching show very similar features. This further demonstrates that the similarity in principle between the streamline-based assisted and automatic history matching.

Field Example 2. This second example is a geologically complex sandstone reservoir consisting of several different facies. The reservoir lies between an underlying shale and an overlying shallow marine shale-siltstone. The reservoir itself is a structural trap (**Fig. 22**). The erratic distribution of sandstones and intervening shales indicate that the depositional environment was transitional and most likely associated with or part of a deltaic environment.

The simulation model has 156 wells, 200×65×40 grid blocks (520,000 cells), and 28 years of production history.[5] Among the 156 wells, 83 producers which had significant water-cut response were used for production data integration purpose. There are inactive cells in the model, and aquifer support was modeled by large porosity values along the periphery. Five different relative permeability zones are used. The reservoir was under primary depletion for an extended period of time, followed by peripheral water-injection. The water-cut responses from the initial permeability model significantly deviate from the history. After 10 iterations by automatic history matching, most of the wells exhibit a much better history match. Some typical wells are shown in **Fig. 23**. After inversion, both shift-time misfit and water-cut misfit were reduced by about half (**Fig. 24**).

Fig. 25 compares the permeability before and after the history match. For most of the 40 layers, the changes are hard to discern by visual comparison (**Fig. 25c**). This is primarily because the streamline-based sensitivities help target the changes to regions of maximum impact. Although some layers show obvious change, the general trend of the static geologic model is retained. We can see that in some areas, permeabilities are reduced (e.g., **Fig. 25a**), while for some regions, permeabilities are increased (e.g., **Fig. 25b**). We also observed that some high permeability channels are created (e.g., **Figs. 25b,d**), while some low permeability barriers are formed (e.g., Fig. 25d). It is reasonable for automatic history matching to form high permeability channel and low permeability barrier for a deltaic depositional environment. Also from the histogram comparison (**Fig. 26**), we can see that the heterogeneity is increased in the updated model. This is reasonable considering the erratic distribution of sandstones and intervening shales and the depositional environment. Both the low values and the high values are further extended, and the artifacts from high permeability cut-off in the initial model seem to have disappeared in the updated model. For this example, it took about 17 hours for IBM Regatta workstation with 10 inversion iterations and less than one week including the setup time for the entire history matching process.

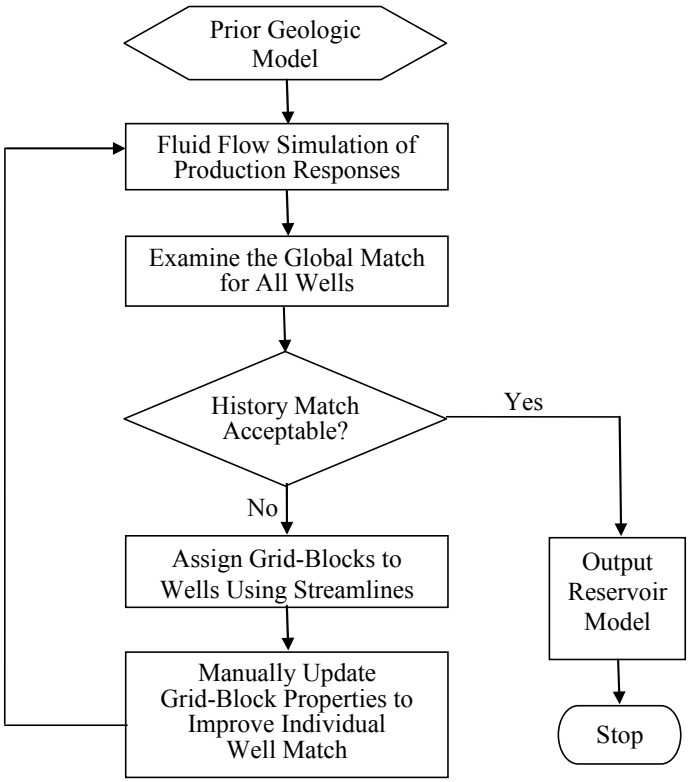

Fig. 1 − Flowchart for assisted history matching.

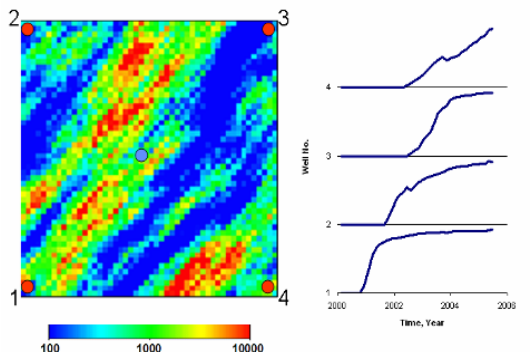

Fig. 2 − Reference permeability field and water cut responses. responses.

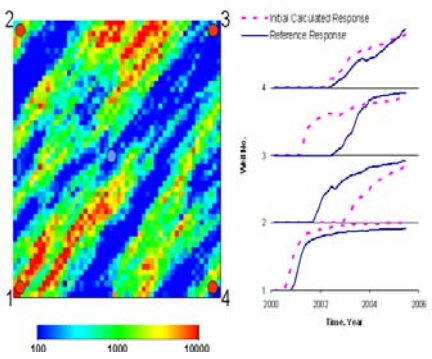

Fig. 3 − Initial permeability field and water cut responses.

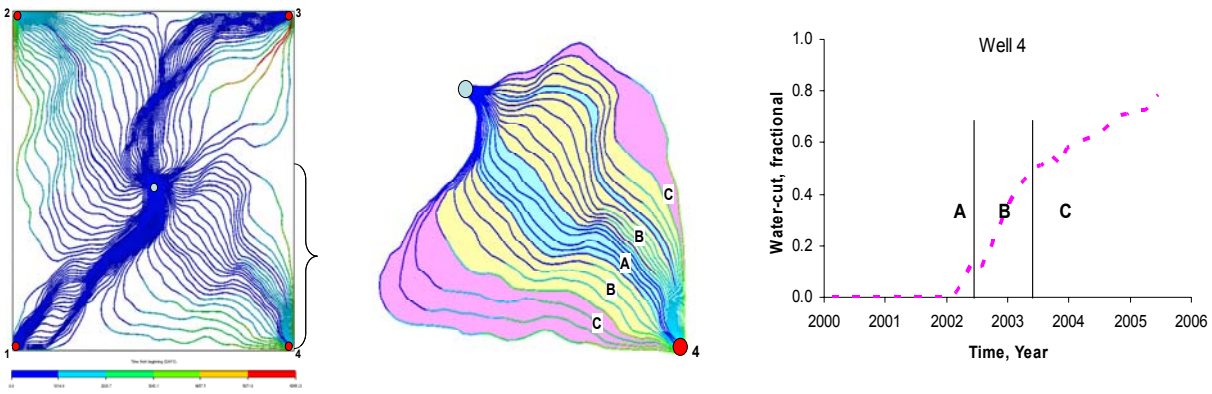

Fig. 4 − Illustration of streamline-based assisted history matching water-cut response.

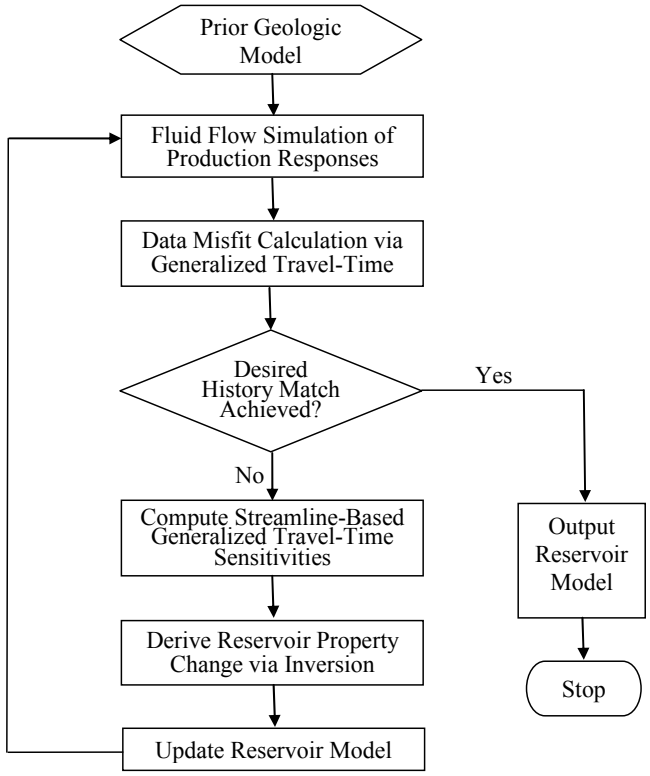

Fig. 5 − Flowchart for automatic history matching.

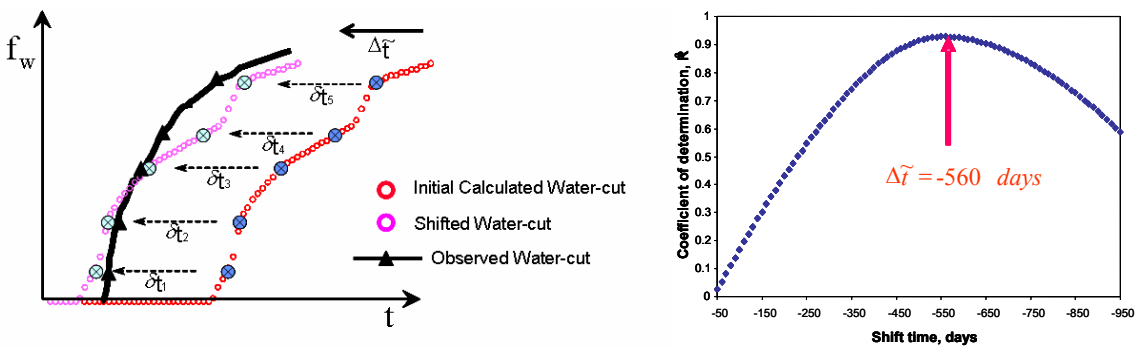

Fig. 6 − Illustration of generalized travel time misfit, correlation function, and generalized travel time sensitivity calculation.

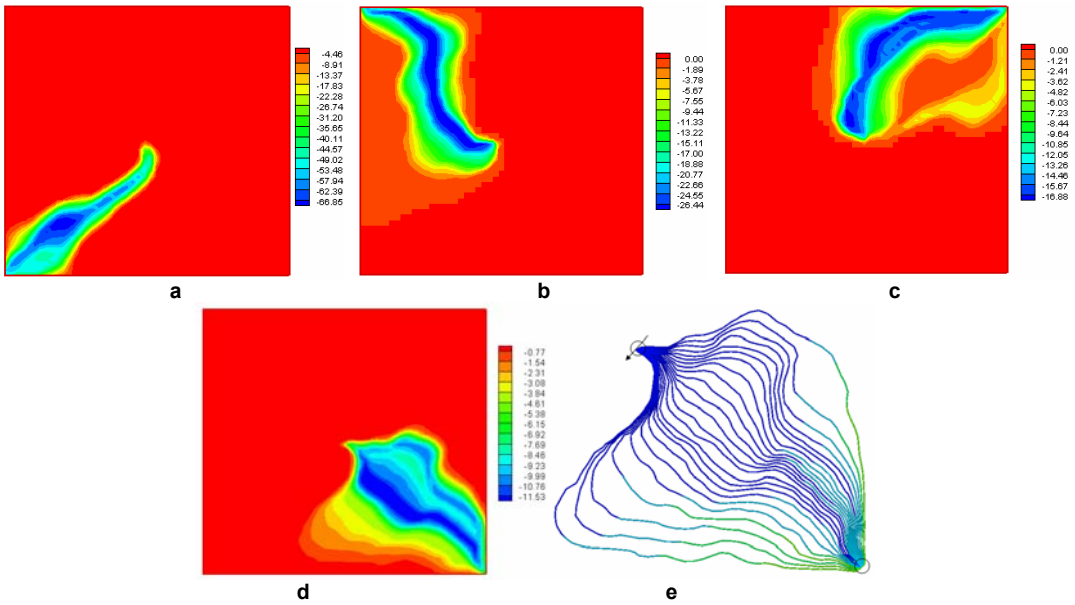

Fig. 7 − Generalized travel time sensitivities for (a) Well 1, (b) Well 2, (c) Well 3, (d) Well 4, and (e) streamlines associated with Well 4.

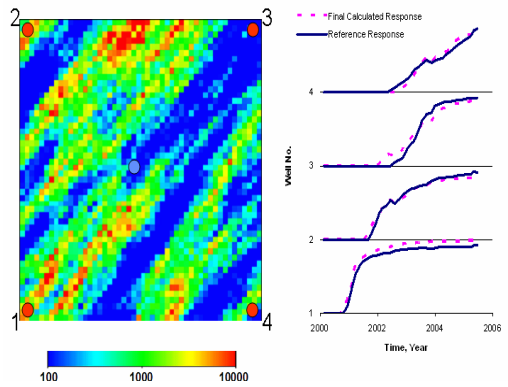

Fig. 8 − Updated permeability field and water cut matches.

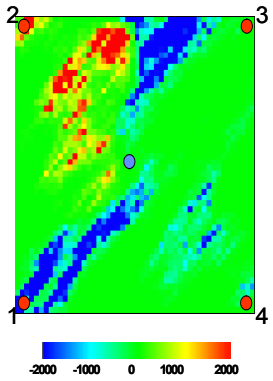

Fig. 9 − Permeability changes.

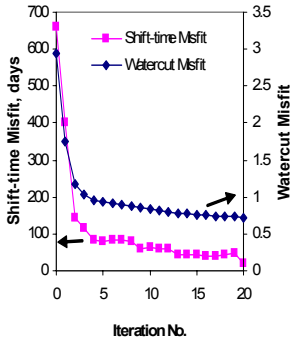

Fig. 10 − Misfit reduction.

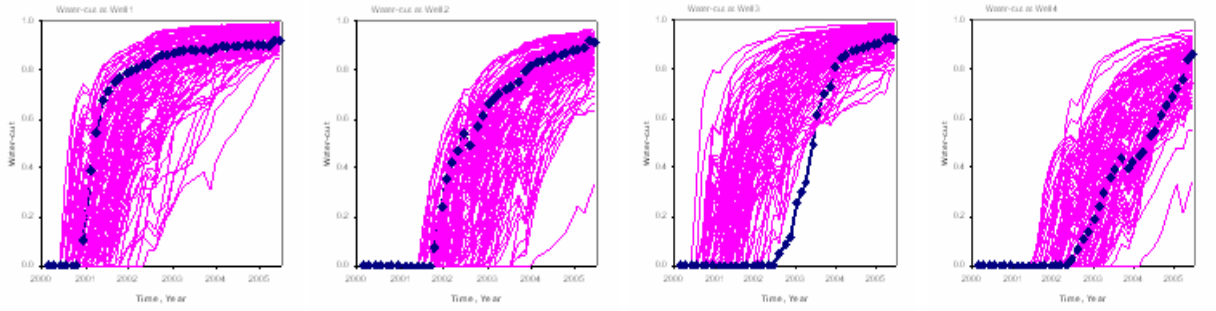

Fig. 11 − Water cuts of four producers from 100 initial realizations together with the results from the reference field (blue squares).

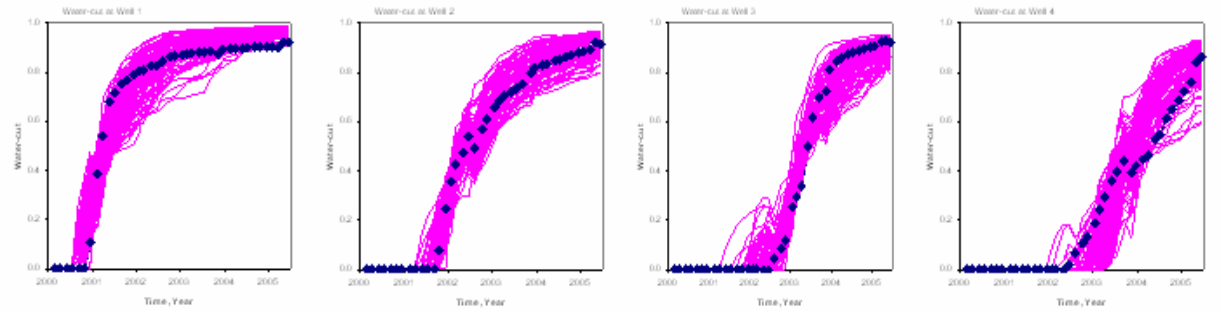

Fig. 12 − Water cuts of four producers from 100 updated realizations together with the results from the reference field (blue squares).

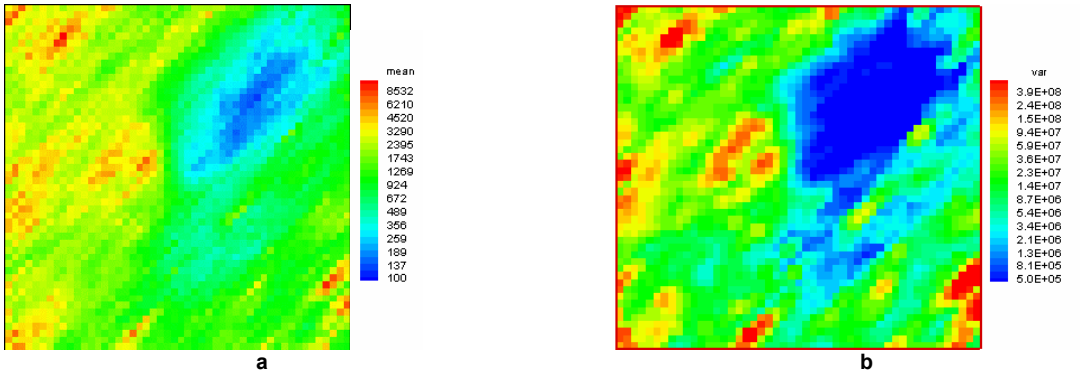

Fig. 13 − (a) Ensemble mean of the 100 final estimated permeability fields and (b) uncertainty in terms of the variance.

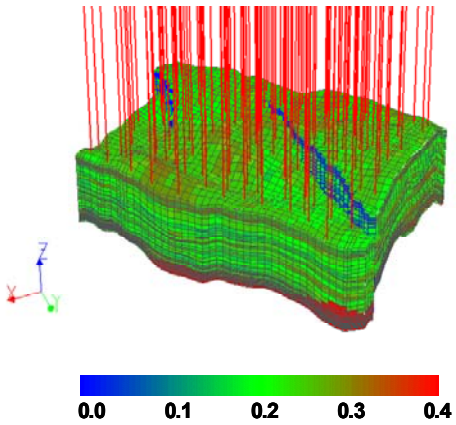

Fig. 14 − Porosity distribution and well locations for BBCK model.

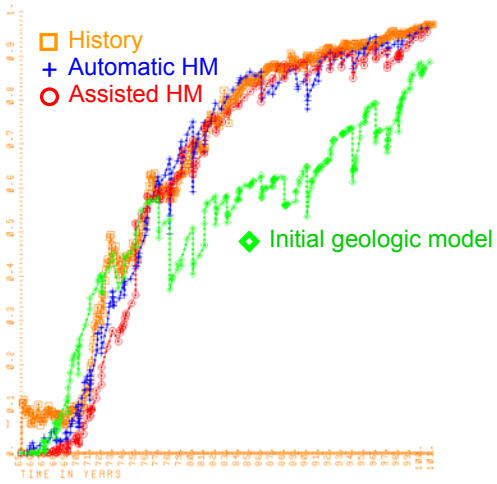

Fig. 15 − Field-wide water-cut performance for BBCK model. Orange-square is the history, green-diamond is static geologic model result, red-circle is assisted history matching result, and blue-plus is the final result by automatic history matching.

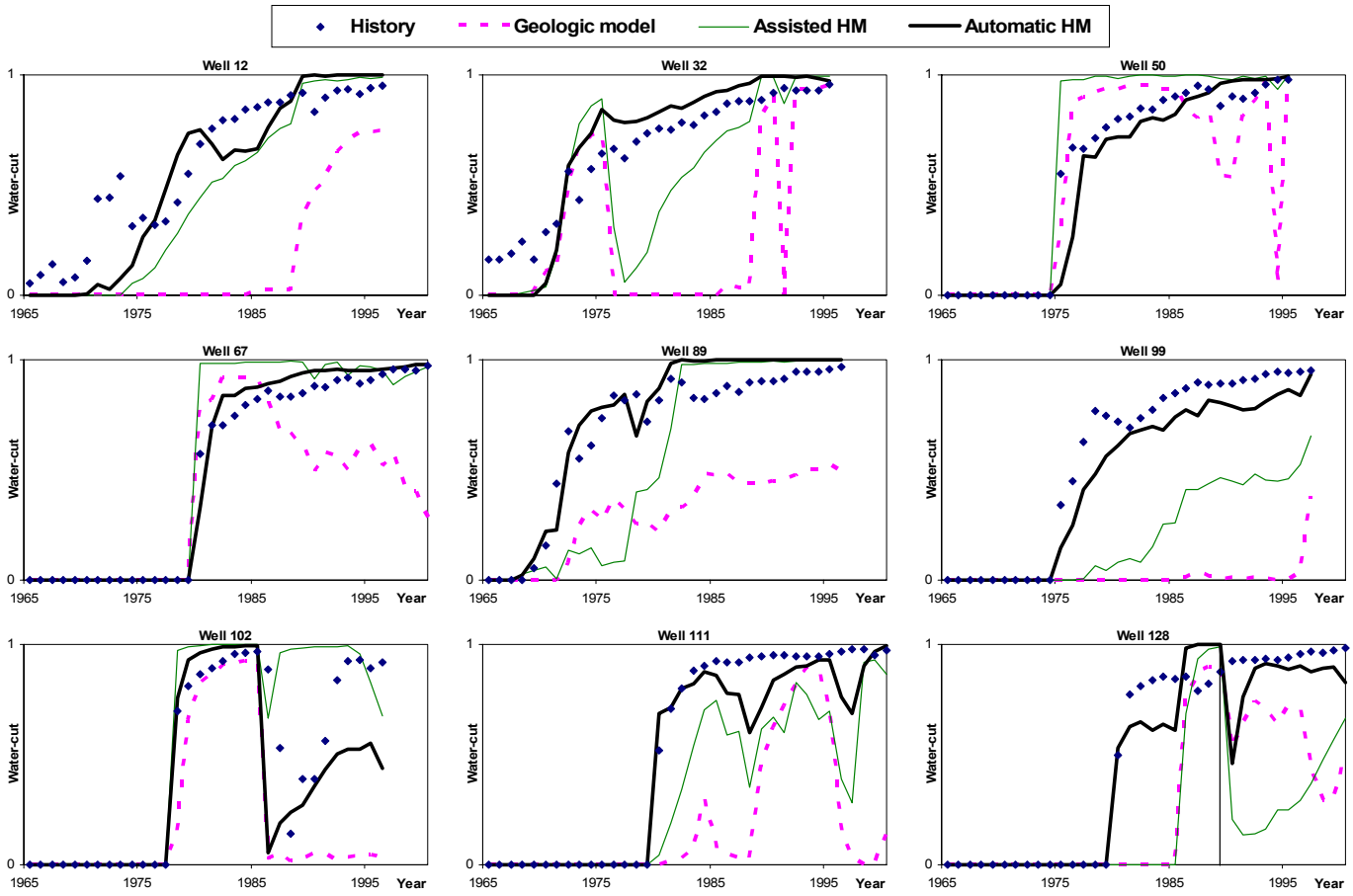

Fig. 16 − Comparison of water cut match by automatic and assisted history matching. 'Diamond' is history, 'red dotted line' is initial static geologic model result, 'green line' is assisted history matching result, and 'black bold line' is final result by automatic history matching. For some wells we matched only part of the data and did prediction for the rest of the production time using the updated model to further validate the model. For example, we matched the data only to Year 1989 for Well 128 (before the black vertical line), and the prediction for the rest of time improved a lot compared to the initial model.

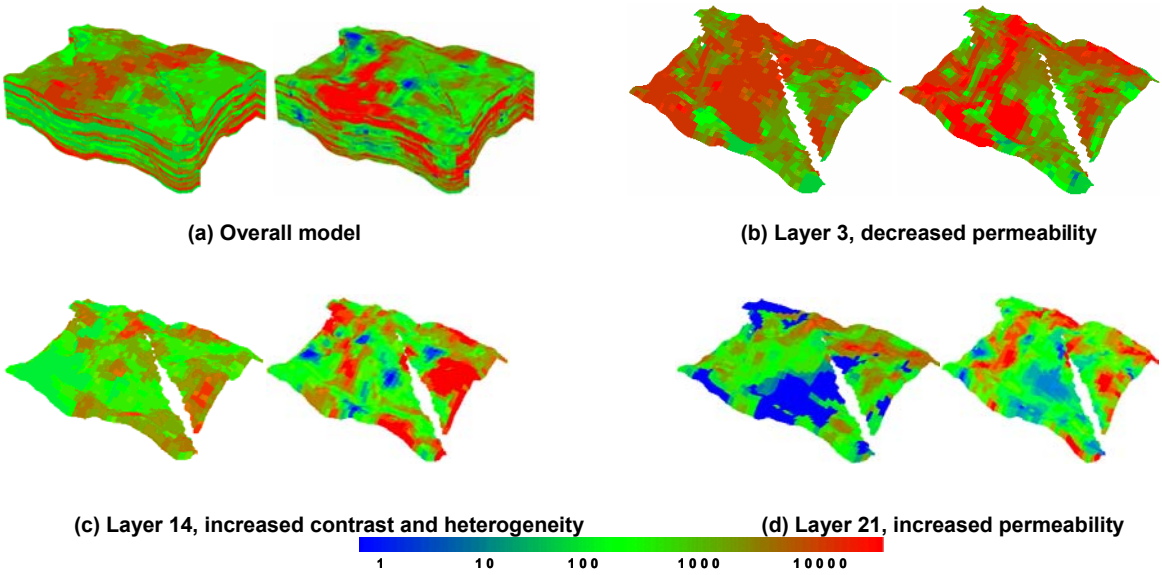

(a) Overall model

(b) Layer 3, decreased permeability

(c) Layer 14, increased contrast and heterogeneity

(d) Layer 21, increased permeability

Fig. 17 − Horizontal permeability distribution of initial static geologic model (left side of each group) and the final inverted model by automatic history matching starting from the initial static model.

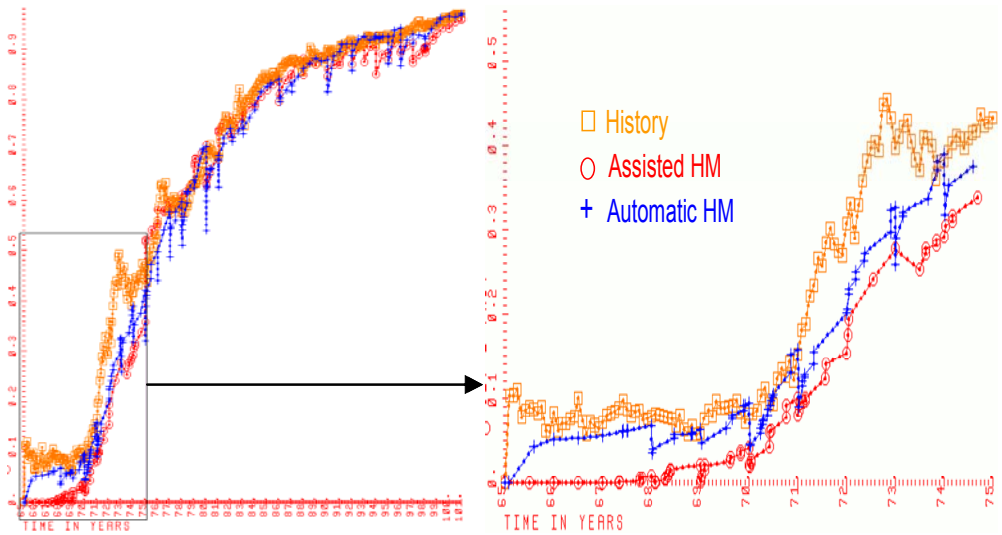

Fig. 18 − Field-wide water-cut performancefor Example 1. Orange-square is history, red-circle is assisted history matching result, and blue-plus is the final automatic history matching result.

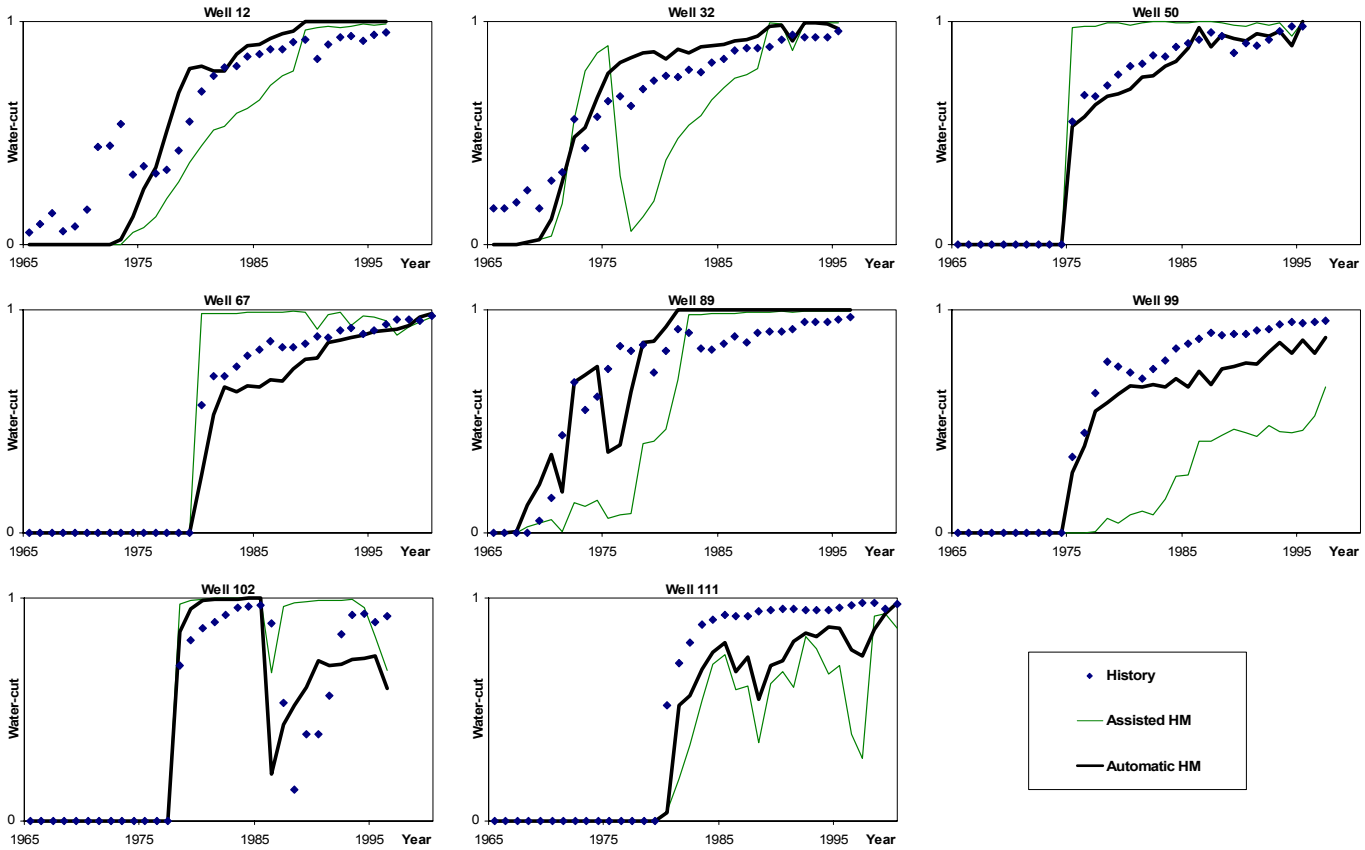

Fig. 19 − Automatic history matching improved water-cut match upon assisted history matching for most of 130 wells. Eight typical wells are shown. 'Diamond' is history, 'green line' is assisted-history-matching result, and 'black bold line' is final result by automatic history matching.

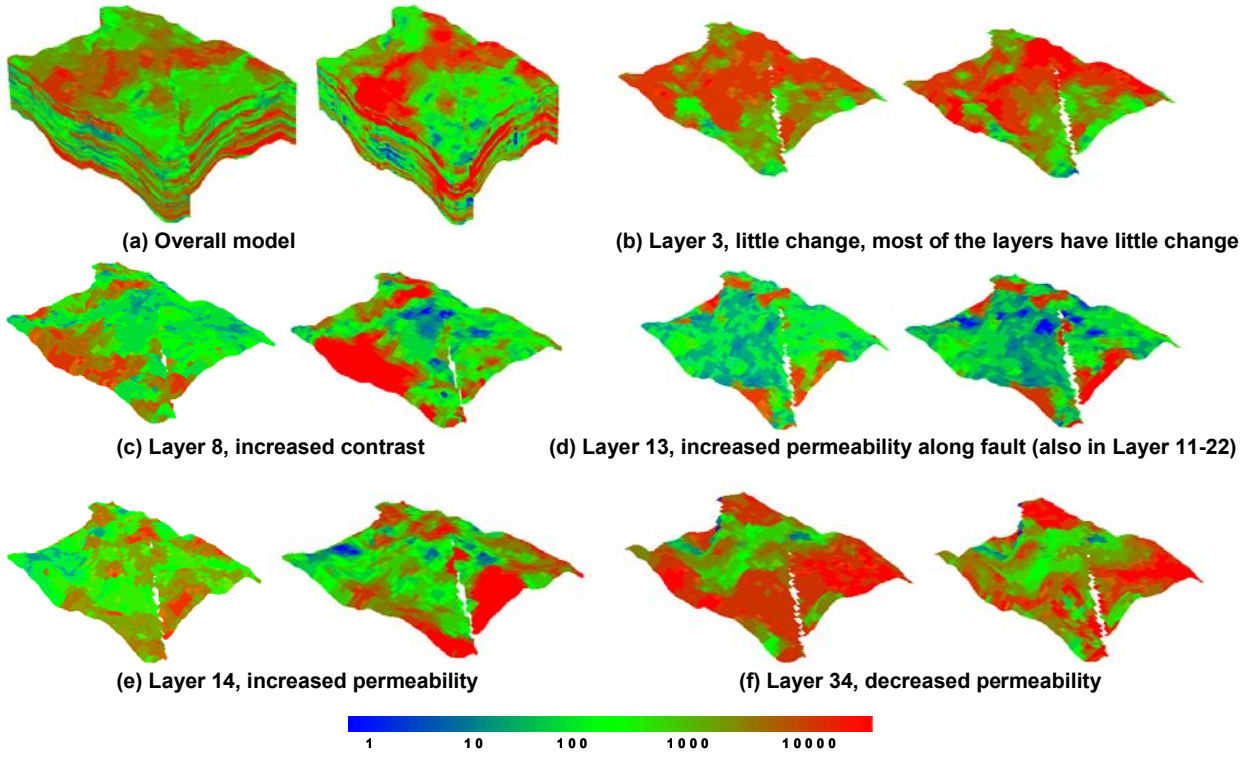

Fig. 20 − Horizontal permeability distribution for assisted history matched model (left side of each group) and automatic history matched model starting from the assisted history matched model for Example 1.

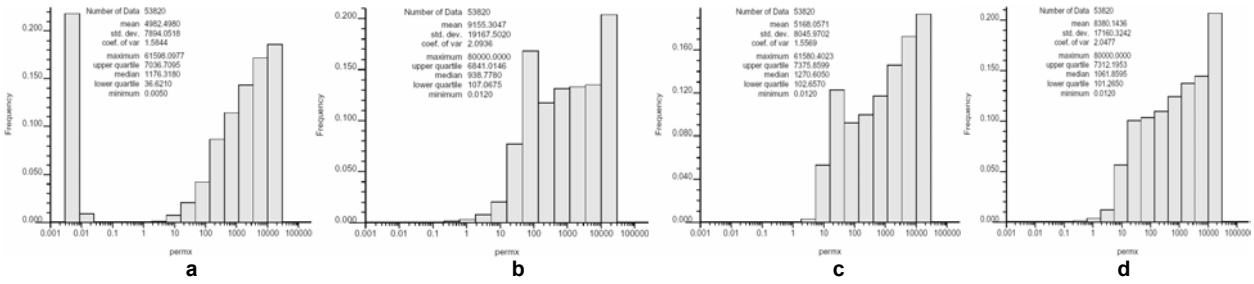

Fig. 21 − Horizontal permeability histogram for (a)static geologic model, (b) final inverted model starting from static model, (c)assisted history matched model, and (d) final inverted model starting from assisted history matched model.

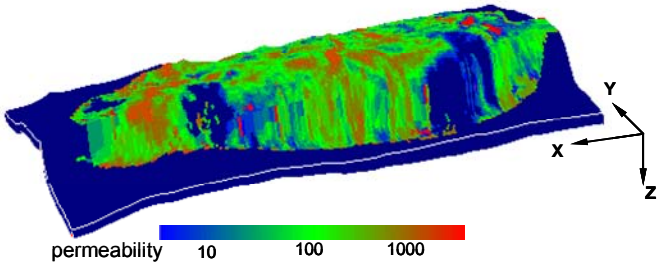

Fig. 22 − Initial static geologic model forExample 2. Dark blue is for inactive regions. Aquifer support was modeled by large porosity values at the periphery. The reservoir itself is a structural trap.

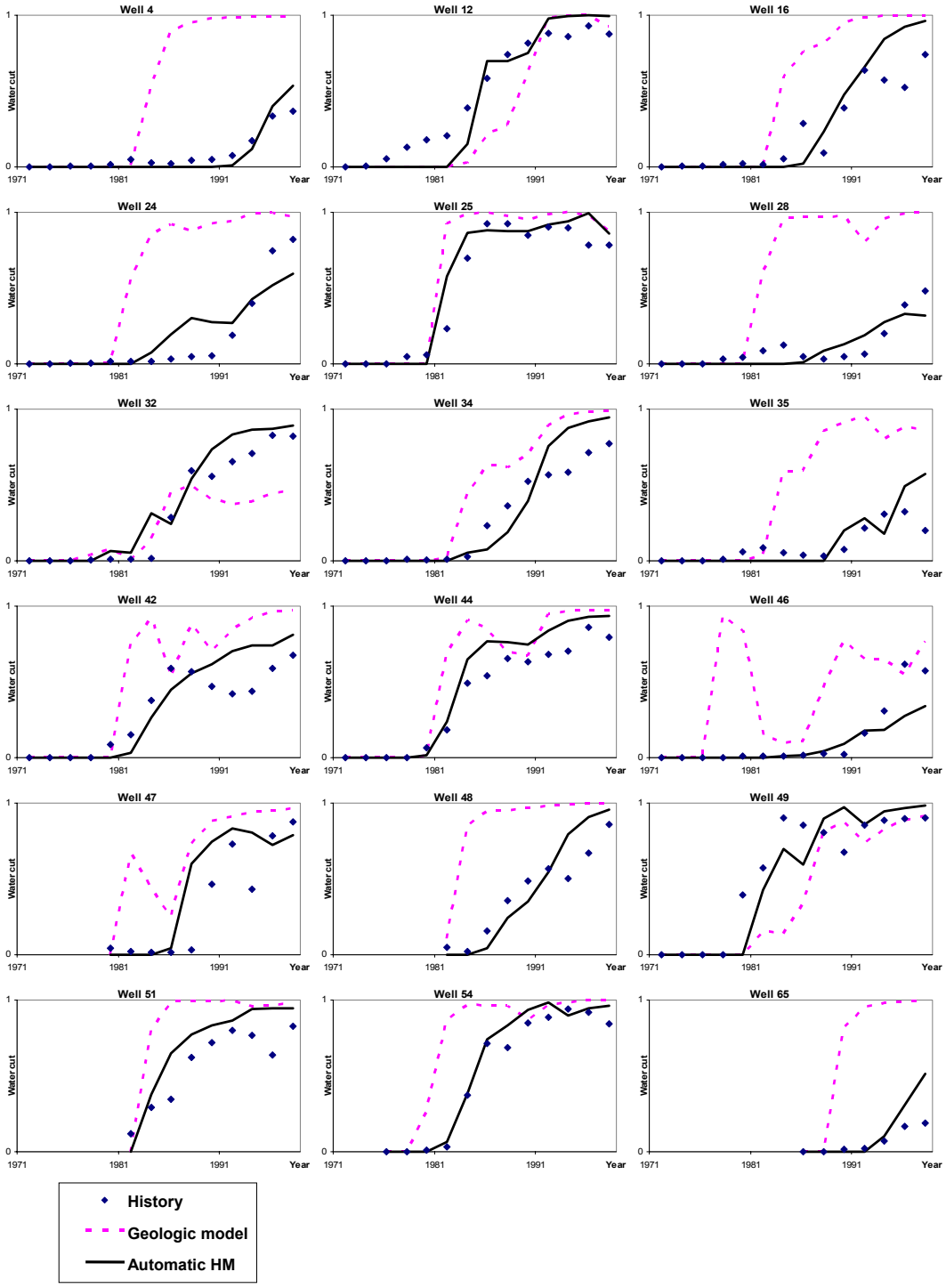

Fig. 23 − Water cut match by automatic history matching for 20 typical wells among 83 wells for Example 2. 'Diamond' is history, 'red dotted line' is initial static geologic model result, and 'black solid line' is final result by automatic history matching.

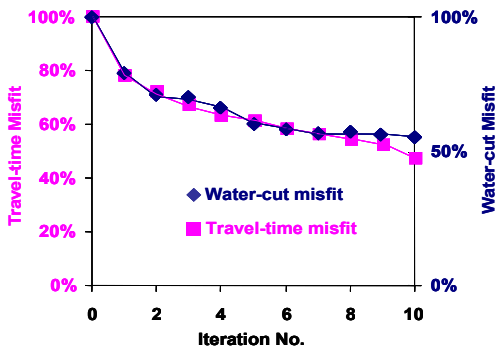

Fig. 24 − Water cut and shift time misfit reduction for Example 2 by automatic history matching.

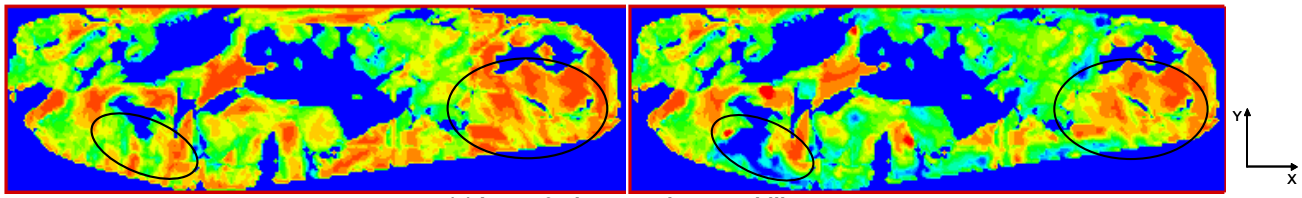

(a) Layer 6: decreased permeability

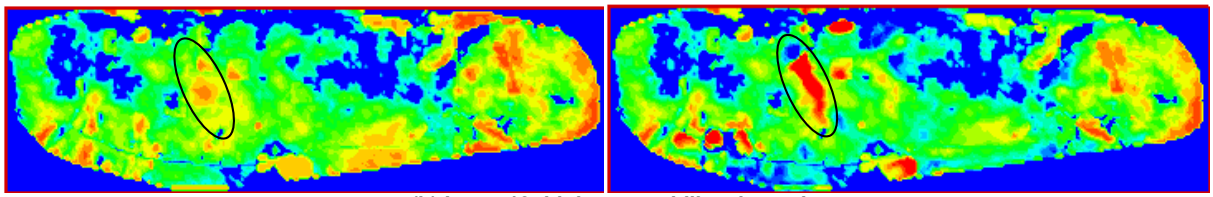

(b) Layer 12: high permeability channel

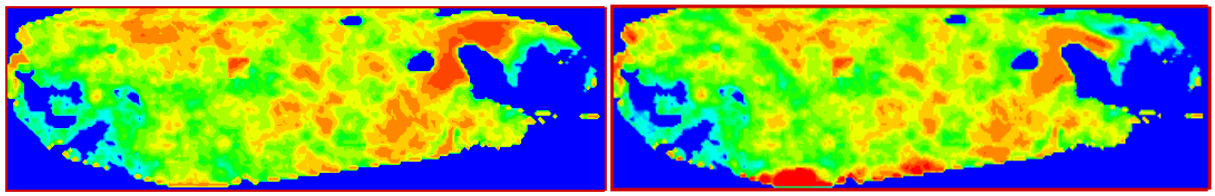

(c) Layer 37: little change

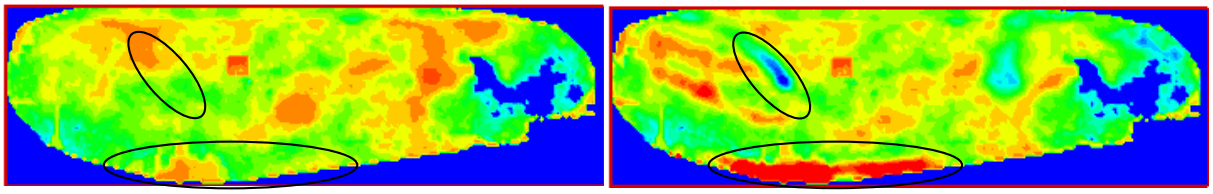

(d) Layer 38: increased permeability at periphery and low permeability barrier

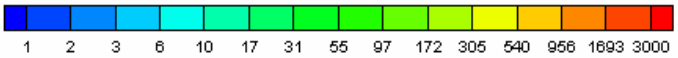

Fig. 25 − Horizontal permeability distribution before (left side of each group) and after automatic history matching for Example 2.

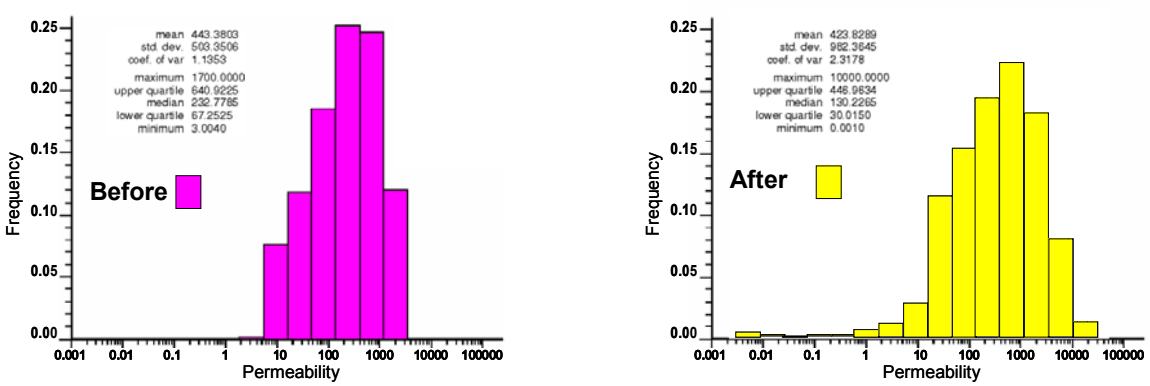

Fig. 26 − Horizontal permeability histogram before and after automatic history matching for Example 2.

RESULTS AND DISCUSSION: PART II

Streamline-Based Production Data Integration in Naturally Fractured Reservoirs

Introduction

Natural fractures are known to play a significant role in subsurface flow and transport of fluids. In recent years, advances in key technologies such as seismic imaging and horizontal drilling revealed the true extent of fractures in many reservoirs and enabled operators to utilize novel ways to use fracture connectivity to enhance recovery. The number of reservoirs that are now considered to be naturally fractured has also risen significantly in recent years and there is a greater need for more robust fracture characterization methods that can integrate both static and dynamic data in an efficient manner.[1]

Of late, discrete fracture network (DFN) techniques have gained increasing attention in the oil industry.[2,3] The DFN is based on mapping fracture planes in 3D space using statistical properties of fracture swarms, fracture network geometry and flow characteristics. The advantage of the DFN models is the ability to incorporate complex fracture patterns based on field data such as cores, well logs, borehole images, seismic data and geomechanics. Although the DFN models can reproduce very realistic fracture geometry, it is important to condition these models to dynamic data such as well test, tracer and production data to reproduce the flow behavior in the reservoir. Such conditioning is particularly important for fractured reservoirs because only a small fraction of the fractures in the DFN model might carry bulk of the fluid flow.[4,5]

Streamline models have shown great potential in integrating dynamic data into high resolution geologic models.[6-10] A unique feature of streamline models has been the ability to efficiently compute the sensitivity of the production data to reservoir parameters such as porosity and permeability. These sensitivities are partial derivatives that quantify how the production response will be affected by changes in reservoir properties. Integrating dynamic data into reservoir models typically involve the solution of an inverse problem and the sensitivities play a key role here. In our previous works, we have utilized the streamline-based sensitivities in conjunction with a generalized travel time inversion method to efficiently integrate production data into geologic models.[7] Our approach has been successfully applied to a large number of field cases including a giant middle-eastern carbonate reservoir.[8]

Until recently, streamline models have been limited to single porosity systems and thus, were not suitable for modeling fluid flow in fractured reservoirs, particularly accounting for matrix-fracture interactions. A common way to model fluid flow in fractured reservoirs is through the dual media approach whereby the fracture and the matrix are treated as separate continua that are connected through a transfer function.[11-13] The transfer functions that describe the exchange of fluids between the matrix and the fracture system can be easily implemented within the framework of the current single porosity streamline models.[14,15] This allows us to utilize much of the techniques related to production data integration developed for single porosity streamline models. However, compared to the single porosity systems, the propagation of the saturation front in the fracture is retarded significantly because of the exchange of fluid with the matrix in dual porosity systems. These effects must be accounted for while computing the travel time sensitivities for saturation fronts. The streamline-derived sensitivities can also be applied in conjunction with dual porosity finite difference simulators and allow us to combine the efficiency of the streamline approach with the versatility of finite difference simulation. The

streamlines can be obtained from the fluid fluxes that are readily available during finite-difference simulation. This significantly broadens the applicability of the streamline-based approach in terms of incorporating compressibility effects and complex physics.[16]

The organization of this report is as follows. First we outline the major steps in our proposed approach and illustrate the procedure using a 2-D synthetic example. Next, we briefly describe the streamline-based dual porosity simulation and how to include matrix-fracture transfer mechanisms within the framework of single porosity streamline simulation. We then describe the extension of streamline-based sensitivity computations to fractured reservoirs and production data integration via generalized travel time inversion. Finally, we demonstrate the power and utility of our method using a realistic 3-D example whereby we use a finite-difference dual porosity simulator and streamline-derived sensitivities to integrate over 20 years of water-cut history.

Approach

Our approach for integrating dynamic data in fractured reservoirs is based on a previously proposed generalized travel time inversion for production data integration.[17] The approach has been shown to be computationally efficient, robust and suitable for large-scale field applications.[7,18] The unique aspect here is the extension and validation of streamline-based analytic travel time sensitivity computations for fractured medium and accounting for matrix-fracture exchange mechanisms. The travel time sensitivities can be applied to both streamline and finite difference simulators. Thus, we can exploit the computational efficiency of the streamline approach and the versatility of the finite difference simulators in terms of handling compressibility and complex physics. The main steps used in our approach are as follows.

- **Dual Porosity Fracture Flow Simulation**. For modeling fluid flow in fractured reservoirs, we can use either a 3D dual porosity streamline simulator or a finite difference simulator. The streamline models have recently been extended to fractured reservoirs using the dual media approach.[14,15] In particular, the dual porosity streamline models can be considerably faster than conventional finite-difference simulators when the primary exchange mechanism between the matrix and the fracture system is capillary imbibition. However, in the presence of strong coupling between the matrix and the fracture system, the streamline models may not offer significant advantage and we revert to conventional finite difference dual porosity flow simulation. The use of finite-difference models allows us to incorporate compressibility and other relevant physical mechanisms without any significant loss in computational efficiency.

- **Generalized Travel-Time and Sensitivity Computations**. The misfit between the observed and computed production response is quantified using a previously proposed generalized travel time.[7,17] A critical aspect of production data integration is calculation of sensitivities that define the relationship between production response and reservoir parameters. We compute these sensitivities analytically as one-dimensional integrals along streamline trajectories. For streamline simulators, these trajectories are readily available. However, for finite difference models an additional step is necessary to compute the streamlines and time of flight based on the finite difference velocity field. These one dimensional calculations scale very favorably with respect to number of grid blocks. Thus, our approach is particularly well-suited for high resolution geologic models.

- **Data Integration Using Generalized Travel Time Inversion**. For history matching, we have used a generalized travel time inversion approach that utilizes the analytical sensitivities is used in conjunction with an iterative optimization scheme to minimize the travel time shift between calculated and observed data.[17] Additional constraints are imposed to integrate prior information and also retain plausibility of the solution. These include a prior covariance model or equivalently a 'roughness' constraint to preserve the spatial correlation of the fracture permeability and a 'norm' constraint to retain the prior geologic features.[17] The generalized travel time inversion has many favorable characteristics including quasi-linear properties that make it attractive for field applications.[7,15]

An Illustration of the Procedure. To illustrate our approach, we will use an example that involves integration of water cut data in a 9-spot pattern. The reference fracture permeability field was derived from a discrete fracture network (DFN) model shown in **Fig 1a**. The model exhibits complex connectivity patterns common to naturally fractured reservoir where the distribution of fracture swarms determines the shape and intensity of fractured regions. A moving window is used to calculate the fracture density for each grid cell which is then converted to a fracture permeability multiplier using a non-linear transform.[20] The fracture permeability is calculated using the multiplier and a predetermined fracture permeability range. The reference fracture permeability distribution is shown in **Fig. 1b.** We used a dual porosity streamline simulator for modeling fluid flow in the fractured medium for this example.

We can randomly extract various percentages of fracture swarms and fractures within the swarms to generate prior models with varying degrees of fracture information. Because production data is more appropriate for characterizing large scale features, fracture swarms location is more critical than the detailed connectivity of individual fractures within a cell. We generate a 2D prior model of fracture patterns by randomly drawing 50% of the fracture swarm and 50% of fractures inside each swarm. **Fig. 2a** shows the prior fracture permeability model.

We match the water cut response from the reference model for the first 500 days using the generalized travel time inversion. Starting with the prior model, we minimize the travel time shift at each producer iteratively to match the reference production data. **Fig. 2b** shows the final fracture permeability model. **Fig 3** shows the observed data, initial model response and the matched response after performing the generalized travel time inversion. The process has not only matched the breakthrough times but also the amplitude of the water cut response for all the wells. Also, **Fig. 2b** shows that after inversion we are able to recover the permeability contrast in the reference model and reproduce the dominant fracture connectivity while retaining most of the features of the prior model. For example, integration of production data has connected the two distinct high permeability regions in the prior model. This is clearly an important feature in the reference model in terms of fluid flow response. Finally, **Fig. 4** shows the convergence of the inversion algorithm. The data misfit is reduced by almost an order of magnitude in only five iterations.

Mathematical Formulation

Dual Porosity Streamline Simulation. Streamline models have recently been generalized to model fluid flow in fractured reservoirs including matrix-fracture interactions.[14,15] A common approach to include such interactions has been through the dual porosity conceptualization whereby the fluid flow is assumed to occur primarily through the high permeability fracture system and the matrix acts as the fluid storage.[11-13] A matrix-fracture transfer function is used to exchange fluid between the matrix and the fracture systems. If we consider incompressible flow in a non-

deformable media, then the conservation equations for the fracture and the matrix in a dual porosity system can be written as follows, [12-15]

$$\phi_f \frac{\partial S_{wf}}{\partial t} + \vec{u}_t \bullet \nabla f_{wf} + \nabla \bullet \vec{G} + \Gamma_w = 0 \quad \text{.....(1)}$$

$$\Gamma_w = \phi_m \frac{\partial S_{wm}}{\partial t} \quad \text{.....(2)}$$

In **Eqs. 1** and **2**, the subscripts *f* and *m* represent the fracture and the matrix systems, respectively. In addition, the fractional flow, f_{wf} and the gravity term, G are defined as follows,

$$f_{wf} = \frac{\lambda_{wf}}{\lambda_{wf} + \lambda_{of}} \quad \text{.....(3)}$$

$$\vec{G} = k \cdot \frac{\lambda_{wf}\lambda_{of}}{\lambda_t}(\rho_o - \rho_w)\vec{g}\nabla D \quad \text{.....(4)}$$

where,

$$\lambda_{wf} = \frac{k_{rwf}}{\mu_w} \quad \text{.....(5a)}$$

$$\lambda_{of} = \frac{k_{rof}}{\mu_o} \quad \text{.....(5b)}$$

$$\lambda_t = \lambda_{of} + \lambda_{wf} \quad \text{.....(6)}$$

We can rewrite **Eq. 1** in terms of the streamline time of flight coordinate by introducing the coordinate transformation[21],

$$\vec{u}_t \cdot \nabla = \phi \frac{\partial}{\partial \tau} \quad \text{.....(7)}$$

where the time of flight τ is the transit time of a neutral tracer along a streamline,[22]

$$\tau = \int \frac{\phi}{\|u_t\|} \partial\zeta \quad \text{.....(8)}$$

The saturation equation for the fracture system, **Eq.1**, now takes the following form,

$$\frac{\partial S_{wf}}{\partial t} + \frac{\partial f_{wf}}{\partial \tau} + \frac{\nabla \bullet \vec{G}}{\phi_f} + \frac{\Gamma_w}{\phi_f} = 0 \quad \text{.....(9)}$$

Eq. 9 together with the matrix saturation **Eq. 2** describes the streamline transport equations for the dual porosity system.

It is important to note that because the fluid flow occurs only in the fracture system, we need to trace streamlines only for the fractured medium. The tracing of streamlines for the dual porosity system is identical to that of the single porosity system.[23] The form of the pressure equation remains unchanged when the primary transfer mechanism between the matrix and the fracture system is counter-current imbibition and the transfer terms cancel out. The transfer function for counter-current imbibition can be described by the following,[14,15,24]

$$\Gamma_w = F_s k_m \frac{\lambda_{wf}\lambda_{om}}{\lambda_{wf} + \lambda_{om}}\left(P_{cm} - P_{cf}\right) \quad \text{.....(10)}$$

The basic steps for streamline simulation in a DPSP system can be summarized as follows: (1) Starting with the fracture permeability field (**Fig. 5a)**, source/sink configuration and boundary conditions, a pressure field is generated as in conventional finite-difference simulation (**Fig. 5b**) (2) Next, the velocity distribution in the reservoir is obtained using Darcy's law and the streamlines are traced using the Pollock approach[23] (**Fig. 5c**). The time of flight or travel time along streamlines are also obtained at this stage and the isochrones represent the front propagation (**Fig. 5d**) (3) The fracture saturation distribution is obtained by solving the 1-D saturation **Eq. 9** (without the gravity term) along each streamline as shown in **Fig. 6a**. Gravity effects can be accounted for in the same manner as in single porosity streamline simulation viz. using operator splitting techniques.[25] **Fig. 6b** shows the saturation distribution along a streamline as a function of matrix-fracture transfer rate in **Eq. 10**. For $F_s = 0$, there is no interaction with the matrix and the solution reverts back to the single porosity formulation. Clearly, the net effect of the matrix-fracture transfer function is to retard the water saturation front in the fracture system. The matrix saturation equation is solved along the streamline at the same time and is shown in **Fig. 6c**. (4) The matrix and fracture saturations are then mapped back onto the grid (**Fig. 6e** and **6f**). Again, the rapid propagation of the saturation front in the fracture system in the absence of transfer to the matrix ($F_s = 0$) can be clearly seen in **Fig. 6d**. (5) The streamlines may be updated to account for changing well conditions such as infill drilling, rate changes etc. As in single porosity simulation, fracture and matrix saturations are mapped from streamlines onto the grid before each update, followed by pressure solution, streamline generation and re-initialization.

Generalized Travel Time Inversion. Production data integration via generalized travel time inversion has three major elements to it: representation of the data misfit, relating production data with reservoir parameters via sensitivities and history matching and model updating via an optimization procedure. We briefly discuss these steps here.

Data Misfit Calculation. The first step in the production data integration approach is quantification of the data misfit. We define a 'generalized travel time' at each well for this purpose. In this approach, we seek an optimal time-shift Δt at each well so as to minimize the production data misfit at the well.[17] This is illustrated in **Fig. 7a** where the calculated water-cut response is systematically shifted in small time increments towards the observed response and the data misfit is computed for each time increment. The optimal shift will be given by the Δt that minimizes the misfit function,

$$J = \sum_{i=1}^{Nd} \left[y^{obs}(t_i + \Delta t) - y^{cal}(t_i) \right]^2 = f(\Delta t, m) \quad \cdots\cdots\cdots\cdots\cdots\cdots \quad (11)$$

Or, alternatively maximizes the coefficient of determination given by the following

$$R^2(\Delta t) = 1 - \frac{\sum \left[y^{obs}(t_i + \Delta t) - y^{cal}(t_i) \right]^2}{\sum \left[y^{obs}(t_i) - \overline{y^{obs}} \right]^2} \quad \cdots\cdots\cdots\cdots\cdots (12)$$

Thus, we define the generalized travel time as the 'optimal' time-shift $\Delta\tilde{t}$ that maximizes the R^2 as shown in **Fig. 7b**. It is important to point out that the computation of the optimal shift does not require any additional flow simulations. It is carried out as a post-processing at each well after the calculated production response is obtained from flow simulation. The overall production

data misfit can now be expressed in terms of a generalized travel time misfit at all wells as follows

$$E = \sum_{j=1}^{Nw} (\Delta \tilde{t}_j)^2 \quad \text{.....(13)}$$

The generalized travel time approach has been successfully applied to many field cases. Furthermore, it leads to a robust and efficient inversion scheme because of its quasi-linear properties.[7,17]

Analytic Sensitivity Computation and Verification. One of the important advantages of the streamline approach is the ability to analytically compute the sensitivity of the generalized travel time with respect to reservoir parameters, for example, fracture permeability. These sensitivities form an integral part of our data integration algorithm.

We have seen that during generalized travel time computation we shift the entire fractional flow curve by a constant time. Thus, every data point in the fractional-flow curve has the same shift time, $\delta t_1 = \delta t_2 = \cdots = \Delta \tilde{t}$ (**Fig. 7a**). We can average the travel time sensitivities of all data points to obtain a rather simple expression for the sensitivity of the generalized travel time with respect to reservoir parameters *m* as follows,[7]

$$\frac{\partial \Delta \tilde{t}_j}{\partial m} = -\frac{\sum_{i=1}^{N_{dj}} \left(\partial t_{i,j} / \partial m \right)}{N_{dj}} \quad \text{.....(14)}$$

All that remains now is to calculate the sensitivity of the arrival times of various water-cut at the producing well, $\partial t_{i,j} / \partial m$. These sensitivities can be easily obtained in terms of the sensitivities of the streamline time of flight,[7]

$$\frac{\partial t}{\partial m} = \frac{\dfrac{\partial \tau}{\partial m}}{\dfrac{\partial f_w}{\partial S_w}}. \quad \text{.....(15)}$$

In the above expression, the fractional-flow derivatives are computed at the saturation of the outlet node of the streamline.[7] For dual porosity streamline models, the saturation evolution along streamlines in the fractured system is carried out in two steps: a predictor step that involves transport along streamlines (identical to the single porosity calculations) and a corrector step that involves the matrix-fracture exchange as follows,[15]

$$\frac{\partial S_{wf}}{\partial t} + \frac{\partial f_{wf}}{\partial \tau} = 0 \text{ : Predictor} \quad \text{.....(16)}$$

$$\frac{\partial S_{wf}}{\partial t} + \frac{\Gamma_w}{\phi_m} = 0 \quad \text{ : Corrector} \quad \text{.....(17)}$$

The fractional flow in **Eq. 15** is computed after the saturation is updated to account for matrix-fracture exchange. If gravity is included, then an additional updating is required to account for gravity segregation before the sensitivities are computed.[25]

Finally, the time-of-flight sensitivities can be obtained analytically in terms of simple integrals along streamline. For example, the time-of-flight sensitivity with respect to permeability will be given by[6]

$$\frac{\partial \tau}{\partial k(\mathbf{x})} = \int_{\Sigma} \frac{\partial s(\mathbf{x})}{\partial k(\mathbf{x})} dx = -\int_{\Sigma} \frac{s(\mathbf{x})}{k(\mathbf{x})} dx, \quad \text{.....(18)}$$

where the integrals are evaluated along the streamline trajectory, and the 'slowness' which is the reciprocal of interstitial velocity, is given by

$$s(\mathbf{x}) = \frac{\phi(\mathbf{x})}{\lambda_t k(\mathbf{x}) |\nabla P(\mathbf{x})|} \quad \text{.....(19)}$$

Note that the quantities in the sensitivity expressions are either contained in the initial reservoir model or are available after the forward simulation run.

In order to verify our DPSP travel time sensitivity in **Eq. 15** we compared our results with sensitivities obtained by numerical perturbation. For this purpose, we simulated water injection in a quarter five-spot pattern. A dual porosity medium with homogeneous fracture permeability represented by 21x21 grid cells was used for this comparison. We perturbed every grid block permeability by 5%, one grid block at a time and numerically computed the partial derivative of the arrival time of a fixed water cut with respect to permeability. **Fig. 8** shows the results for water cuts of 0.10 and 0.20. Clearly, we obtain a good agreement between analytical travel time sensitivities calculated from **Eq. 15** and numerical travel time sensitivities. The perturbation method shows some artifacts partly because the results depend on the magnitude of perturbation whereas the analytical sensitivities are symmetric and smooth. The differences are also because of the approximations inherent in the analytical computations, particularly the assumption that the streamlines do not shift because of small perturbation in reservoir properties. Nevertheless, as we will see later, the streamline-based sensitivities are adequate for history matching purposes under a wide variety of conditions.

Data Inversion Various approaches have been proposed in the literature for the integration of production data via inverse modeling.[26-30] These can be broadly classified into 'deterministic' and 'Bayesian' methods. Both methods have been successfully applied to history matching of field data. In this work, we have adopted a Bayesian formulation whereby we minimize the following penalized misfit function,

$$\frac{1}{2}(m - m_p)^T C_M^{-1}(m - m_p) + \frac{1}{2}\left[\Delta \tilde{\boldsymbol{t}}\right]^T C_D^{-1}\left[\Delta \tilde{\boldsymbol{t}}\right] \text{.....(20)}$$

In **Eq. 20**, $\Delta\tilde{\mathbf{t}}$ is the vector of generalized travel-time shift at the wells; C_D and C_M are the data error covariance and the prior model parameter covariance, respectively. The minimum in **Eq. 20** can be obtained by an iterative least-squares solution to the linear system[31]

$$\begin{bmatrix} \mathbf{C}_D^{-1/2}\mathbf{G} \\ \mathbf{C}_\mathbf{M}^{-1/2} \end{bmatrix} \delta \mathbf{m} = \begin{bmatrix} \mathbf{C}_D^{-1/2}\left(\Delta\tilde{\mathbf{t}}\right) \\ \mathbf{C}_\mathbf{M}^{-1/2}\left(\mathbf{m_p} - \mathbf{m}\right) \end{bmatrix}. \quad \text{.....(21)}$$

where G is the sensitivity matrix containing the sensitivities of the generalized travel time with respect to the reservoir parameters and m_p represents the prior model. We use an iterative sparse matrix solver, LSQR, for solving the augmented linear system in **Eq. 21**. The LSQR

algorithm is well suited for highly ill-conditioned systems and has been widely used for large-scale tomographic problems in seismology.[32]

An important consideration in the solution of **Eq. 21** is calculation of the square-root of the inverse of the prior covariance matrix. We have used a numerical stencil that allows for an extremely efficient computation of $C_M^{-1/2}$ and is applicable to a wide range of covariance/variogram models.[33]

Application and Results

In this section we demonstrate the feasibility of our approach for field studies by application to a large-scale 3-D example. For modeling fluid flow in the reservoir we have used a commercial finite-difference simulator (ECLIPSE[34]) for this case. The dual porosity two phase model used is completely general and accounts for all relevant mechanisms such as fracture-matrix transfer, compressibility, gravity and capillary effects and other cross-streamline fluxes. As mentioned before, we use streamlines and time of flight derived from the finite difference simulator to compute the sensitivity of the production data with respect to reservoir parameters. It is important to note that we do not need to solve the 1-D transport equations along streamlines for computing the sensitivities. Instead, the saturation of the outlet block from the finite difference solution is used directly to compute the fractional flow derivative in **Eq. 15**. This makes the sensitivity computation very fast even for finite-difference simulators and the additional work required involves only streamline generation, computation of the time of flight and the solution of 1-D integrals along streamlines to compute the travel time sensitivities. We must emphasize here that the streamline-derived sensitivities are only approximate, particularly in the presence of compressible flow and strong matrix-fracture coupling. Nevertheless, our experience shows these sensitivities are adequate for inversion purposes and do not have any noticeably adverse impact on the convergence of the solution. Our hybrid workflow capitalizes on the strengths of the two approaches to make fracture flow inversion efficient and at the same time broadly applicable. A flow chart depicting the outline of our procedure is shown in **Fig. 9**. There are 4 main steps involved in the iteration loop

- Fluid flow simulation using a dual porosity finite difference simulator.
- Use of finite-difference velocity field to obtain streamlines, time of flight and travel time sensitivities at specified time intervals, particularly at changes in well events.
- Use of generalized travel time to quantify data misfit.
- Iterative minimization for model updating and history matching until convergence.

Large-Scale 3D Example. This synthetic example is designed after a carbonate reservoir in west Texas. The dual porosity reservoir model used here has a mesh size of 58x53x10 with a total of 30,740 grid cells that represent the fracture permeability distribution. To start with, we generated a reference fracture pattern distribution using a discrete fracture network (DFN) model. The DFN model was generated on a layer by layer basis using pre-specified distributions that control fracture length, height, aperture and azimuth inside elliptical fracture swarms. The motivation behind using the DFN model is that we can use fracture parameters derived from seismic lineament maps, image logs, regional stress studies etc. to generate realistic fracture distribution constrained to field data. The discrete fracture pattern was then converted to a continuum model using grid block permeability multipliers as discussed before. **Fig. 10** shows the reference fracture permeability for the ten layers. Clearly, the layers 2, 4, 7 and 9 are highly fractured and will have a significant impact on the flow behavior. For comparison purposes, **Fig. 11** shows the

discrete fracture networks for layers 2, 4 and 7. The fracture permeability varies over three orders of magnitude from a minimum of 2.5 md to a maximum of 1600 md. The matrix permeability was fixed at 1 md.

There are 31 producers and 11 injectors in the model which consist of 11 inverted 5-spot patterns covering 320 acres. The detailed production rates and well schedule including infill drilling, well conversion and well shut-ins can be found elsewhere.[7] **Fig. 12** shows the well locations and the streamlines at the end of 7500 days of simulation. Just as in streamline simulation, we generate the streamlines only when there are significant changes in the well events or boundary conditions. These streamlines are then used to compute the time of flight and travel time sensitivities in **Eq. 15.** For this example we used 11 streamline updates to account for changing well conditions during the sensitivity computations.

For demonstration of our production data integration approach, we will start with two different prior models and match the water-cut history obtained from the reference permeability field. The first model was generated using 50% of the fractures and fracture swarms in the reference fracture distribution (**Fig. 11**). Thus, the prior model contained altogether about a quarter of all the fractures in the reference model. The second model contained 75% of the fracture and fracture swarm information and thus had approximately half of all the fractures in the reference model. The fracture porosity was kept fixed at 0.03.

Prior Model-1: 50% Fracture Information. In this example we retain 50% of the information in the reference fracture pattern (**Fig. 11**). Both the fracture swarm location and the fracture density within the swarms were included as part of the prior information. The discrete fracture pattern generated is shown in **Fig. 13** for layers 2, 4 and 7. The prior permeability distribution is shown in **Fig. 14**. As expected, the prior model exhibits less connectivity and fewer preferential flow paths compared to the reference model. The final permeability field after matching water-cut response at the producers is shown in **Fig. 15**. The water-cut response from the prior model for 30 producers is shown in **Fig. 16**. In the same figure we have superimposed the water-cut response from the reference model. Clearly, we see a large discrepancy in the production response because of the lack of fracture connectivity and permeability contrast in the prior model. After inversion, a close agreement is obtained between the reference and the calculated production response as shown in **Fig. 16**. On comparison of the final permeability field with the reference permeability distribution, we see that we are able identify the dominant flow paths in the reference model through the integration of production data. For example, in layers 2 and 7 (**Fig. 17)**, the inversion process re-establishes the high contrast and recovers some of the connected pathways seen in the reference model. We can see similar effects across many of the layers. However, the results also underscore the inherent non-uniqueness in the solution, particularly in 3-D because of the large degree of freedom for these flow paths. This makes prior information vital to the success of the inversion. Finally, **Fig. 18** shows the convergence of the inversion as a function of number of iterations. Both travel time misfit and overall water-cut misfit are reduced significantly after 20 iterations. The entire history matching took 3.2 hours in a PC (Intel Xeon 3.06 GHz Processor).

Prior Model-2 : 75% Fracture Information. The prior model for this example was generated by retaining 75% of the information regarding fracture swarms and fracture density within swarms. Again, the discrete fracture network generated for layers 2, 4, and 7 are shown in **Fig. 19**. The permeability distribution is shown in **Fig. 20**. As expected, the prior model for this case

shows a closer resemblance to the reference permeability field. This is also reflected in the computed water-cut response shown in **Fig. 22**. Clearly, the production response for this model is much closer to the reference production history compared to the previous model. Although many of the wells show good match, the lack of fracture connectivity and permeability contrast still impacts the production response of several wells, for example, wells 2, 3, 8, 9 and 14, among others. After inversion, we obtain excellent agreement for all wells as shown in **Fig. 22**. The final permeability field after inversion is shown in **Fig. 21.** On closer observation, for example, layers 3 and 5 (**Fig. 23**), we see that we are able to match the production data with minimum deviation from the prior model. This is expected because of the higher fracture information in the prior model. Also the inverse algorithm by design attempts to preserve prior information to maintain geologic realism.[31] **Fig. 24** shows the misfit reduction as a function of the number of iterations for this example. Again, the misfit is reduced by almost an order of magnitude.

Finally, on comparing the results of inversion using the two different prior models, we can clearly see the role of prior information in our ability to predict fluid flow through fractured reservoirs. Although we were able to match the production history reasonably well starting with 50% fracture information, the results improved significantly when additional fracture data were incorporated. This observation is true for inverse modeling in general; however, the impact is expected to be more pronounced for fractured reservoirs because of the high contrast between the fracture and matrix permeability and the role of preferential fracture flow paths on the overall flow behavior. The inverse problem is ill-posed and we can not expect to reproduce the details of the fracture pattern in the reference model. However, we can reduce the non-uniqueness by anchoring the solution close to the prior model. By starting with different prior models and matching different 'realizations' of the production data, we can explore the uncertainty space by sampling from the posterior distribution.[35]

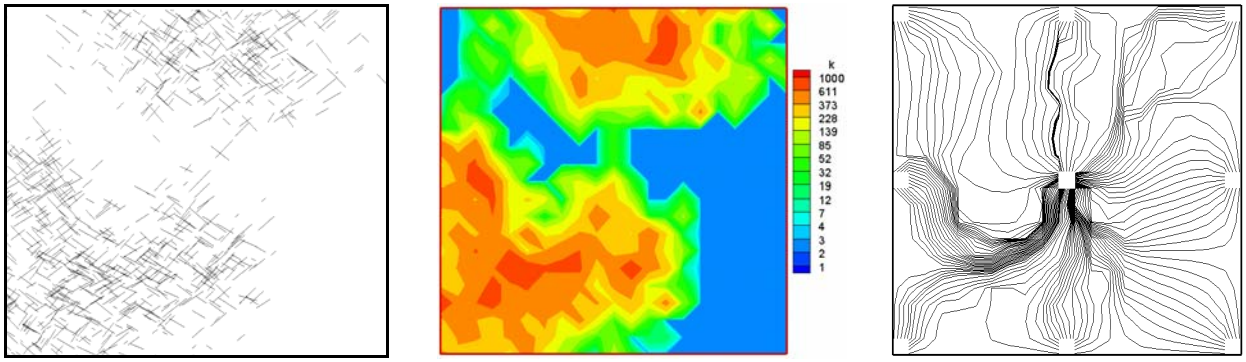

(a) Discrete fracture network (b) Reference fracture permeability (c)Streamline pattern

Fig. 1— Reference model for the 9-spot 2D case

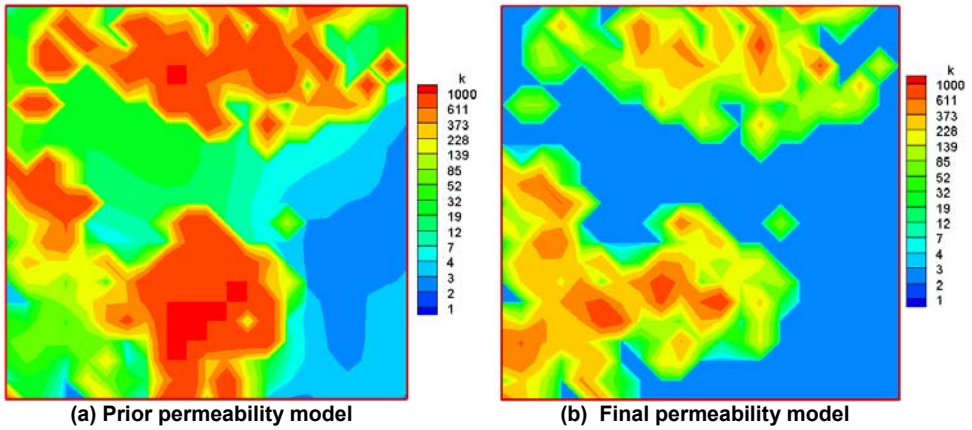

(a) Prior permeability model (b) Final permeability model

Fig. 2— Prior and final permeability models after integrating water cut data.

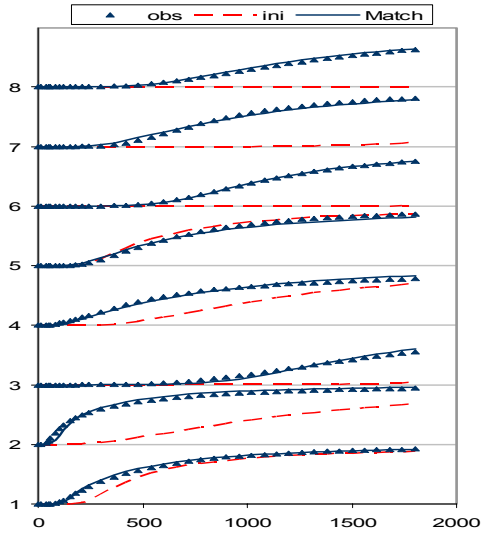

Fig. 3— Initial and final water cut match.

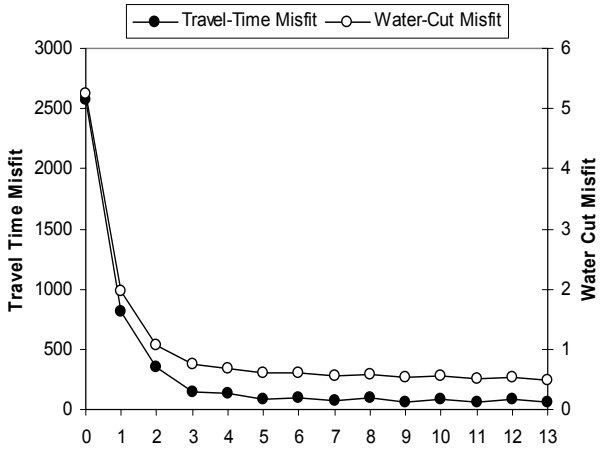

Fig. 4— Data misfit vs. number of iterations.

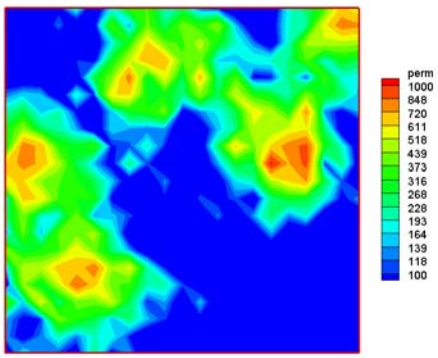

(a) Permeability field

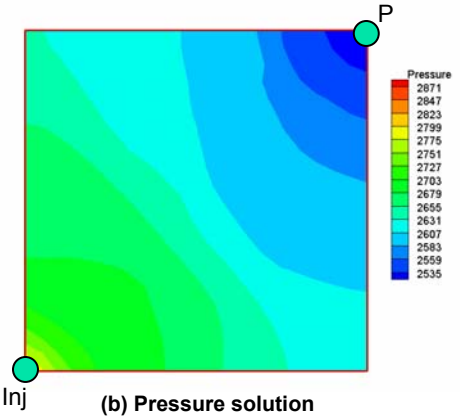

(b) Pressure solution

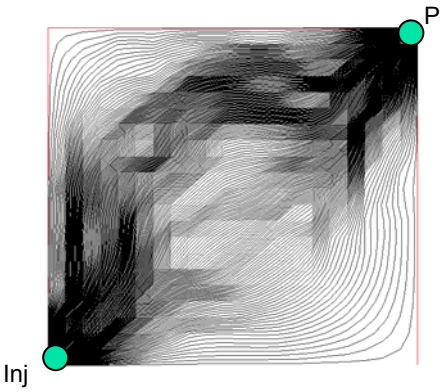

(c) Streamlines

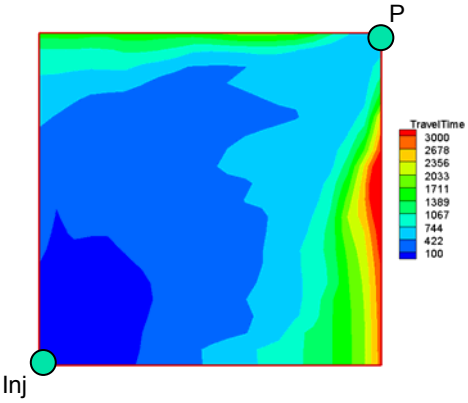

(d) TOF map

Fig. 5— Streamline and time of flight (TOF) calculations.

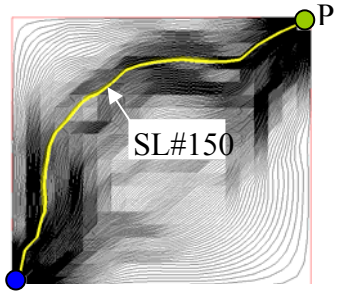

(a) 1-D streamline solution

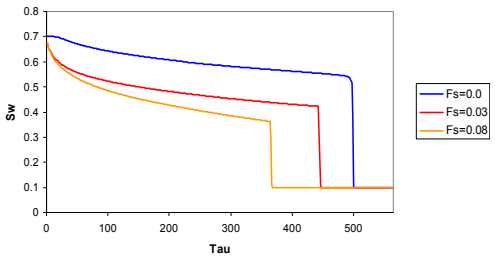

(b) Fracture Saturation

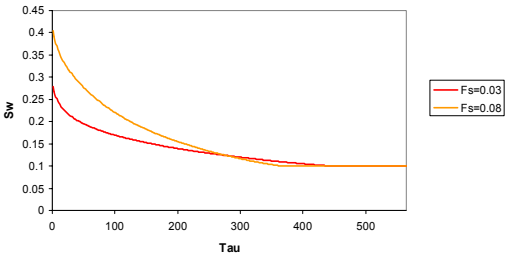

(c) Matrix Saturation

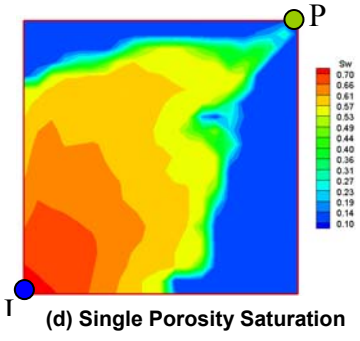

(d) Single Porosity Saturation

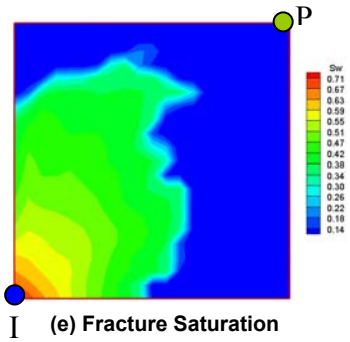

(e) Fracture Saturation

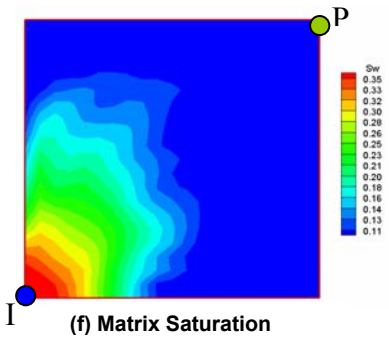

(f) Matrix Saturation

Fig. 6 —Saturation evolution along streamlines – single and dual porosity examples.

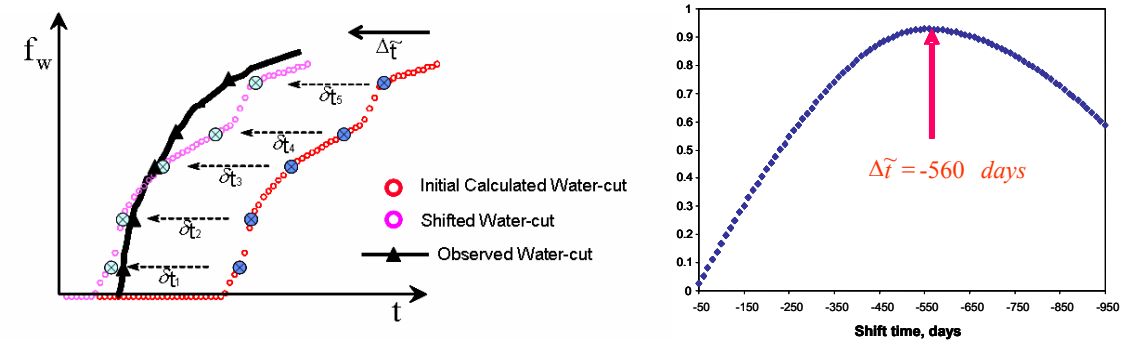

(a) Time shift (b) Maximizing correlation

Fig. 7—Illustration of generalized travel-time inversion: (a) History-matching by systematically shifting the calculated water-cut to the observed history, (b) Best shift-time that maximizes the correlation function.

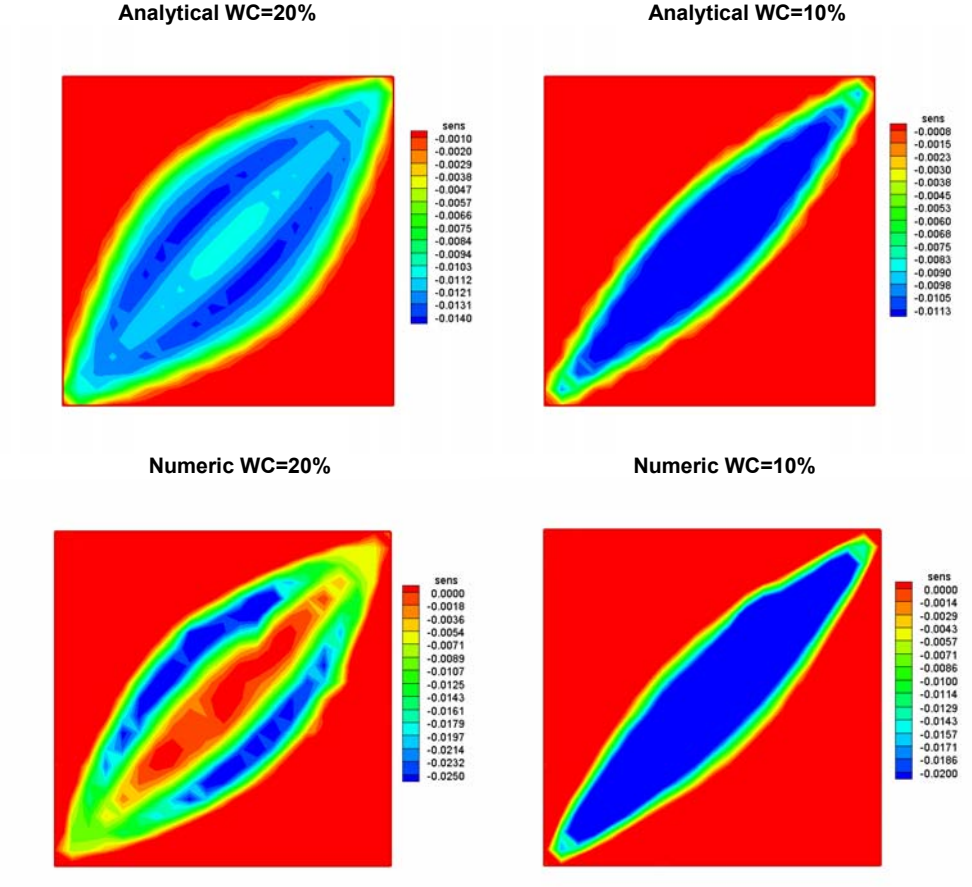

Fig. 8— Comparison of numerical and analytical sensitivities in a ¼-five spot pattern.

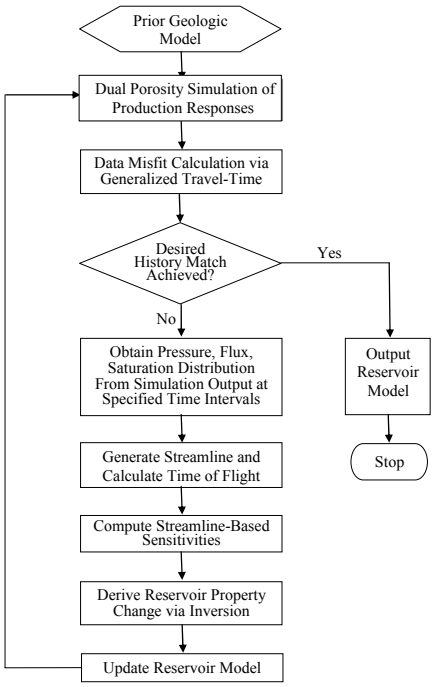

Fig. 9—— Flowchart for history matching dual porosity finite-difference models using streamline-derived sensitivities.

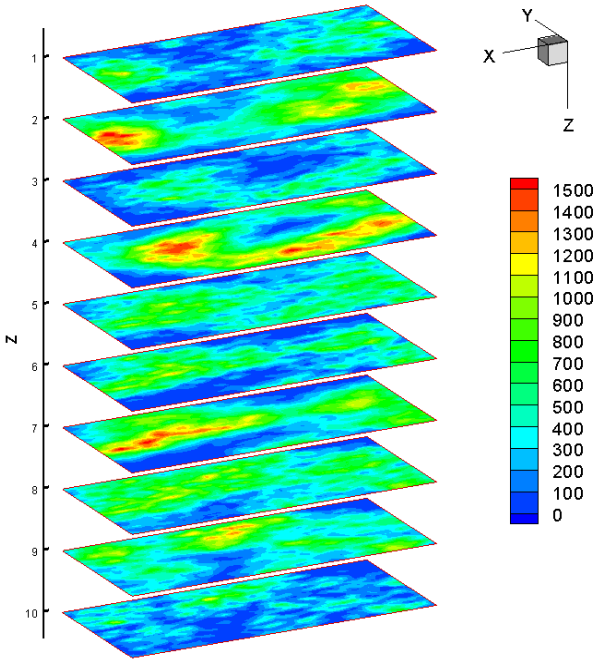

Fig. 10—Reference fracture permeability distribution.

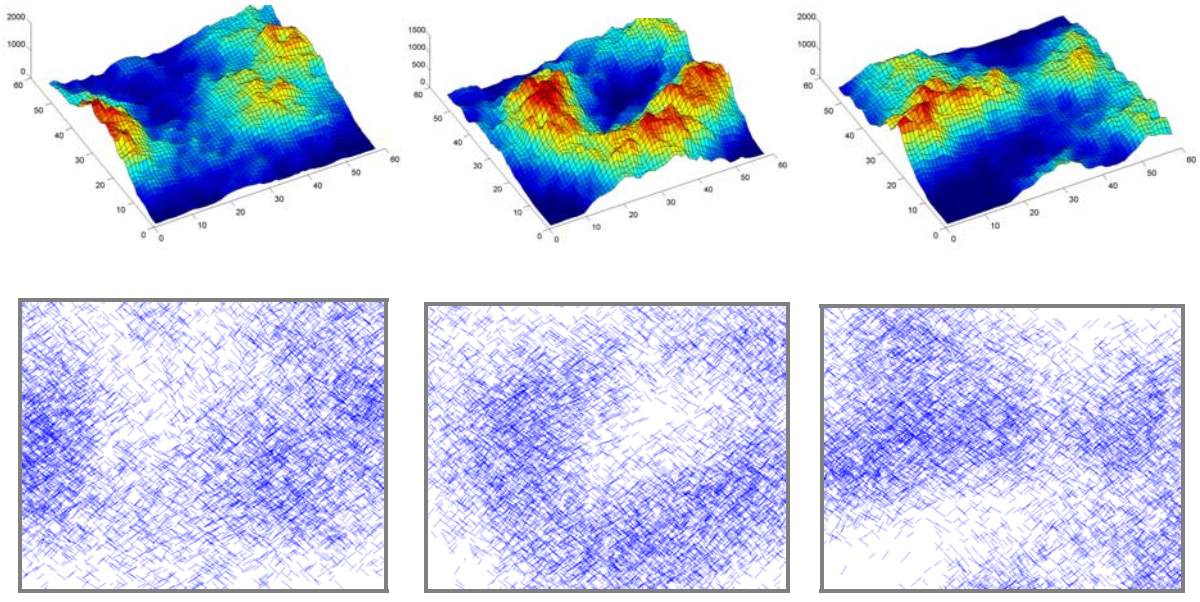

(a) Layer 2 **(b) Layer 4** **(c) Layer 7**

Fig. 11—Discrete fracture layers converted to permeability (upper panel) using fracture intensity

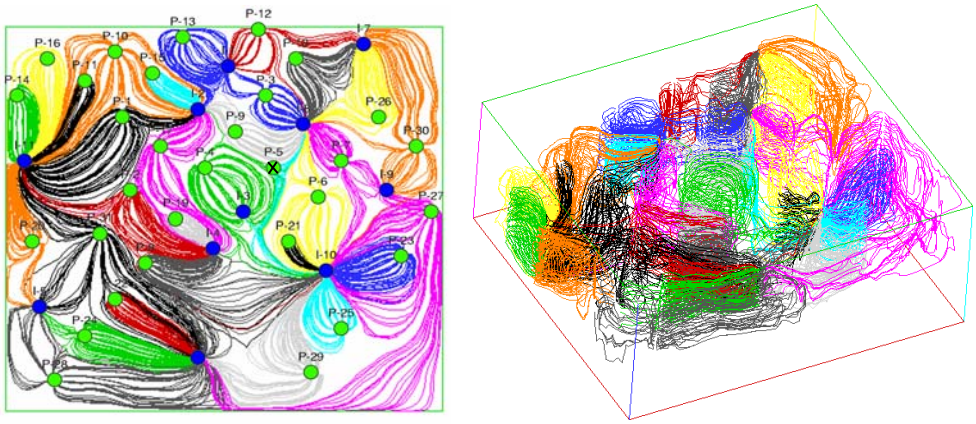

(a) Well locations and streamlines

(b) 3D Streamlines

Fig. 12—(a) Top view shows well locations and streamlines at the end of the last update. (b) 3D streamlines traverse layers in 3D space.

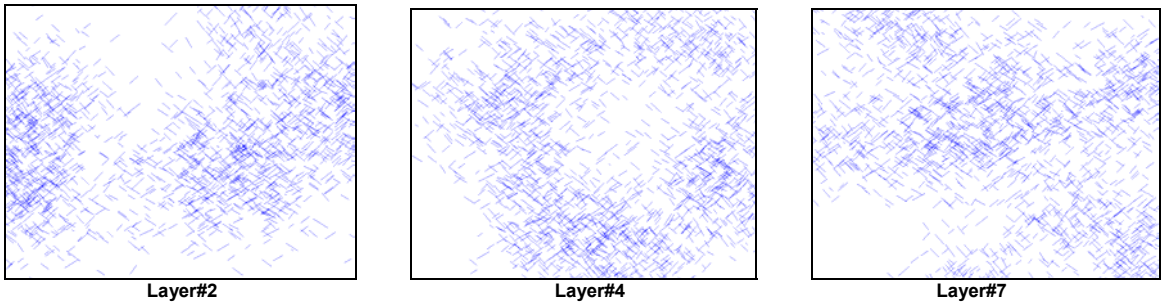

Layer#2 Layer#4 Layer#7

Fig. 13—Discrete fracture networks for 3 different layers with 50% fracture information.

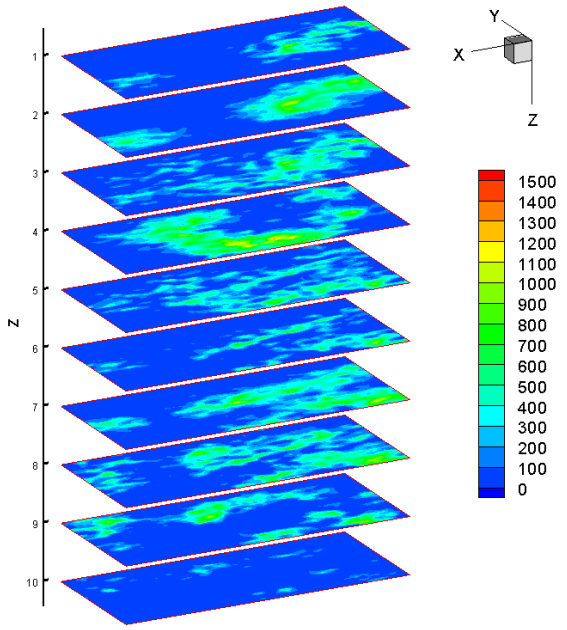

Fig. 14— Permeability distribution for prior model with 50% fracture information.

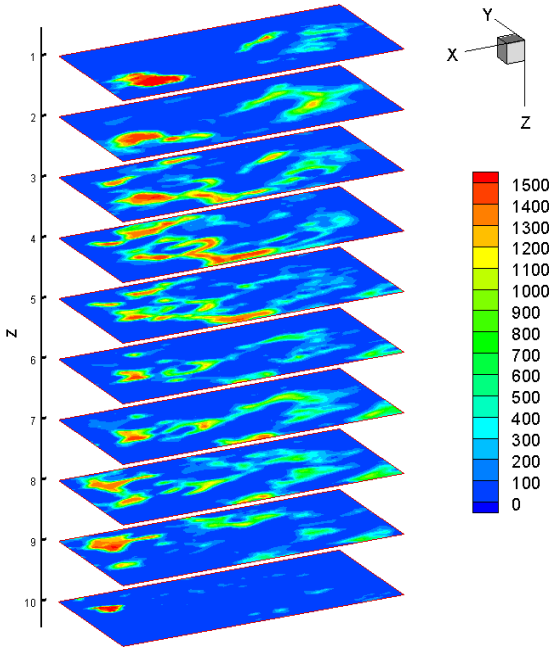

Fig. 15—Final permeability distribution after water cut integration.

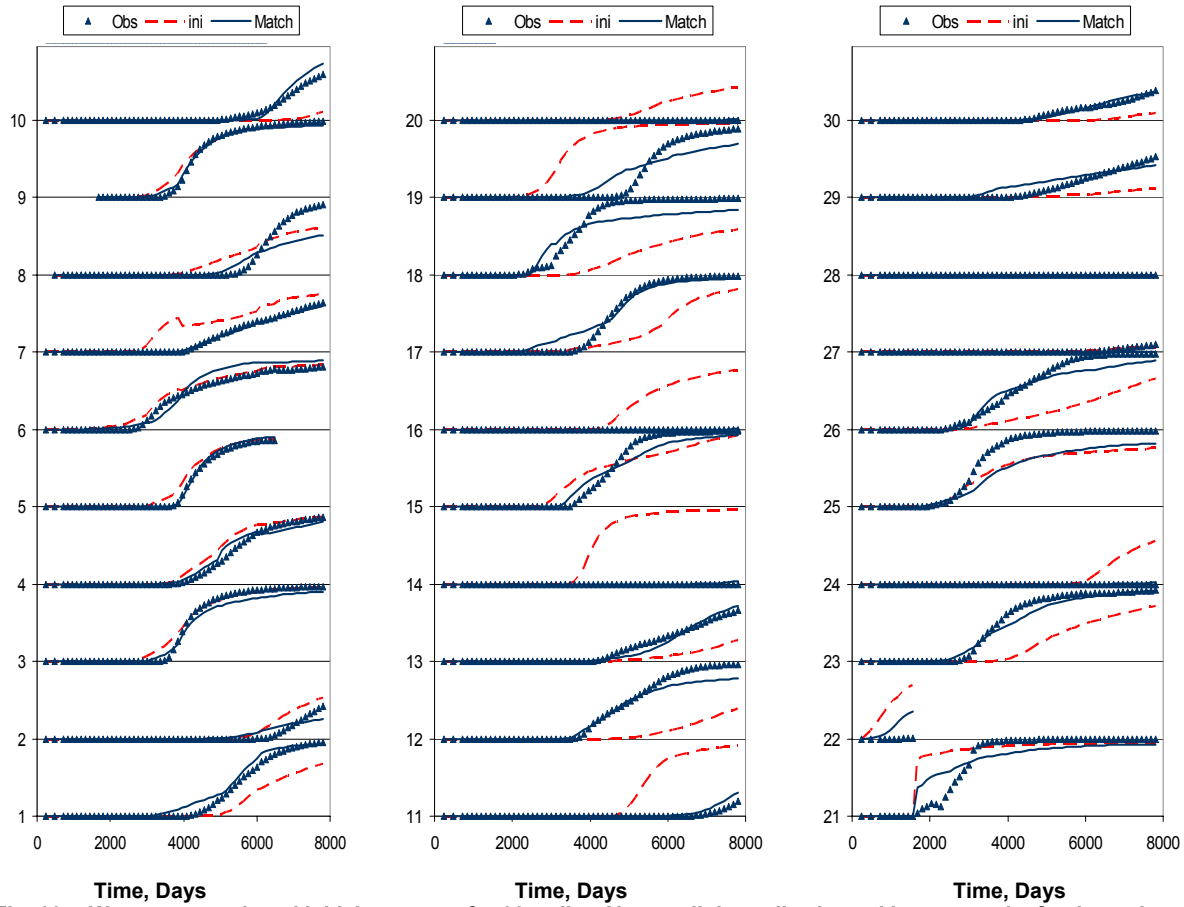

Fig. 16— Water cut match and initial response for 30 wells. Almost all the wells showed better match after inversion.

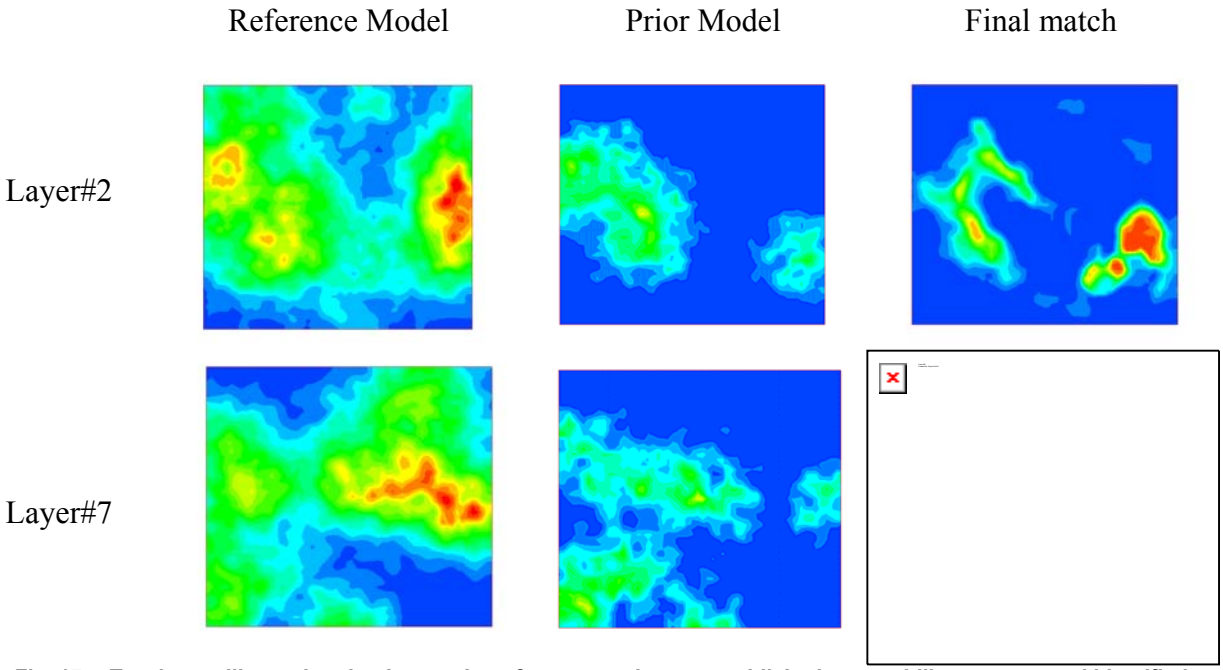

Fig. 17— Two layers illustrating that integration of water cut data re-established permeability contrast and identified major flow paths while preserving the prior information.

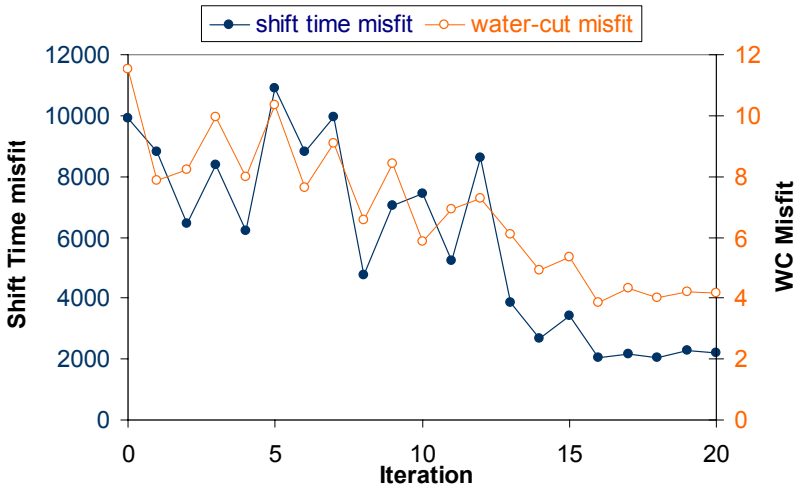

Fig. 18—Data misfit vs. iterations (prior model-1)

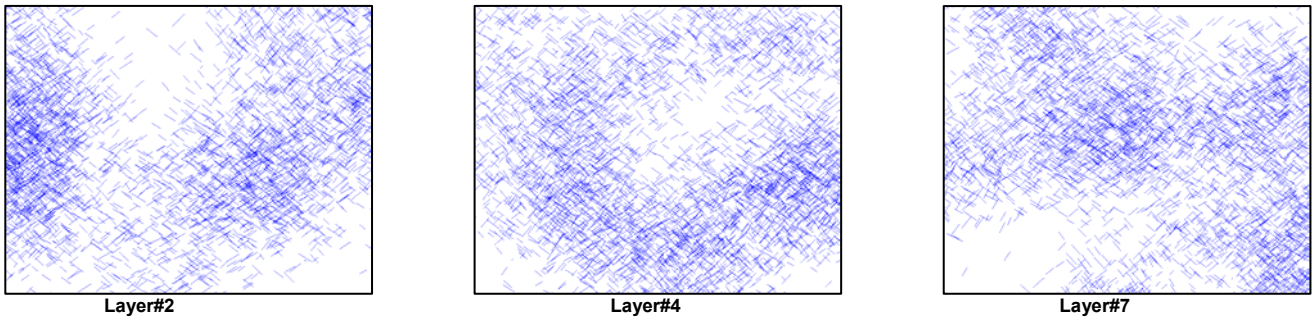

Fig. 19—Discrete fracture network for 3 layers with 70% fracture information

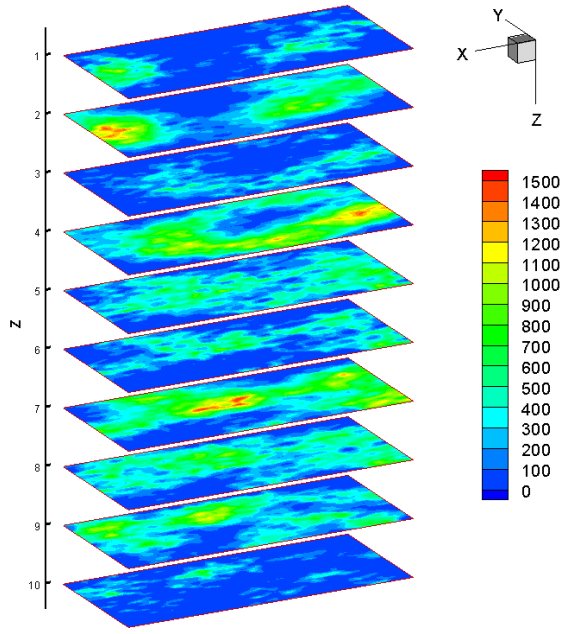

Fig. 20— Permeability distribution for the prior model with 75% fracture information.

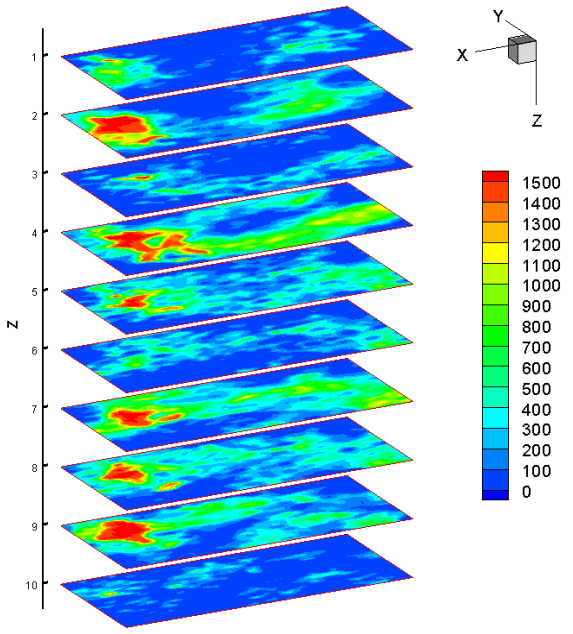

Fig. 21—Final permeability distribution after water cut integration.

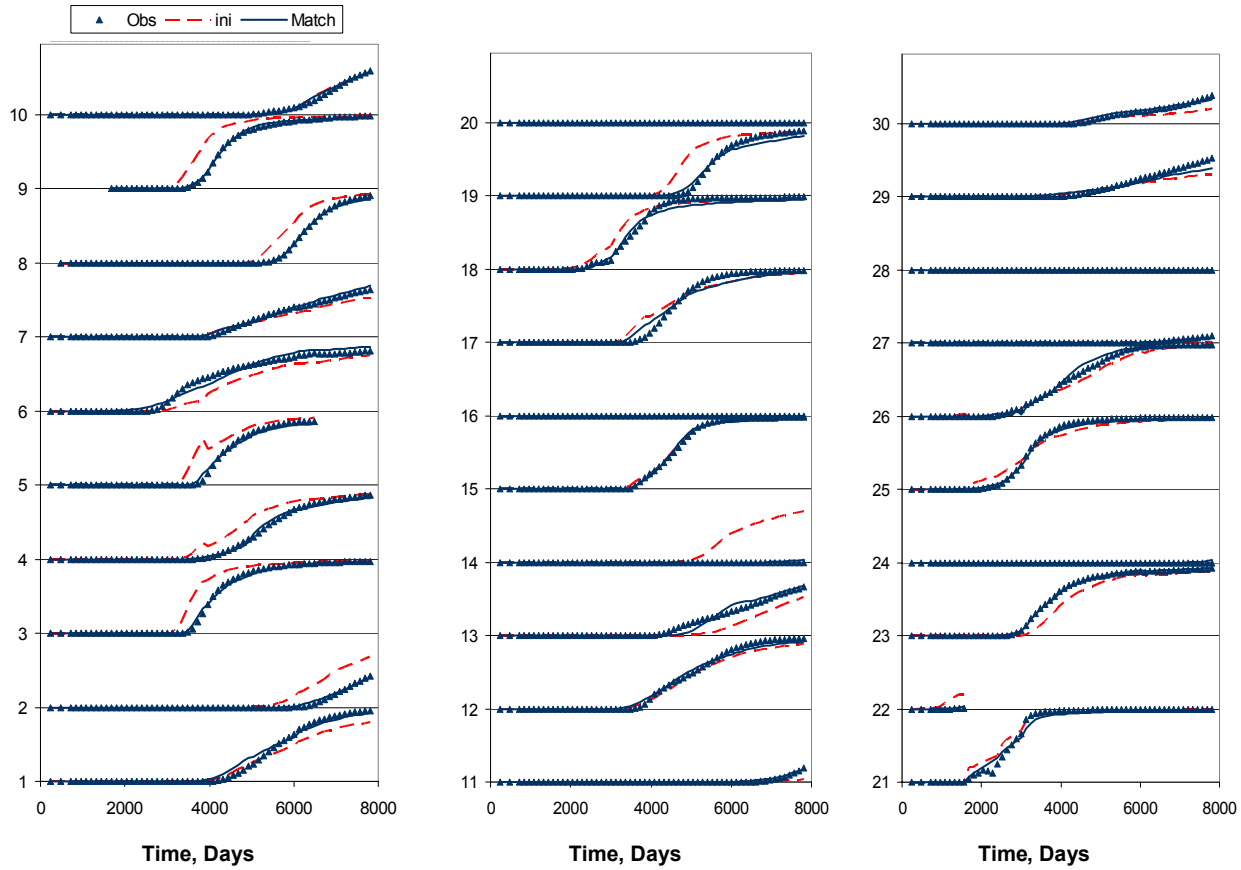

Fig. 22— Water cut Match and initial response for 30 wells for prior model-2.

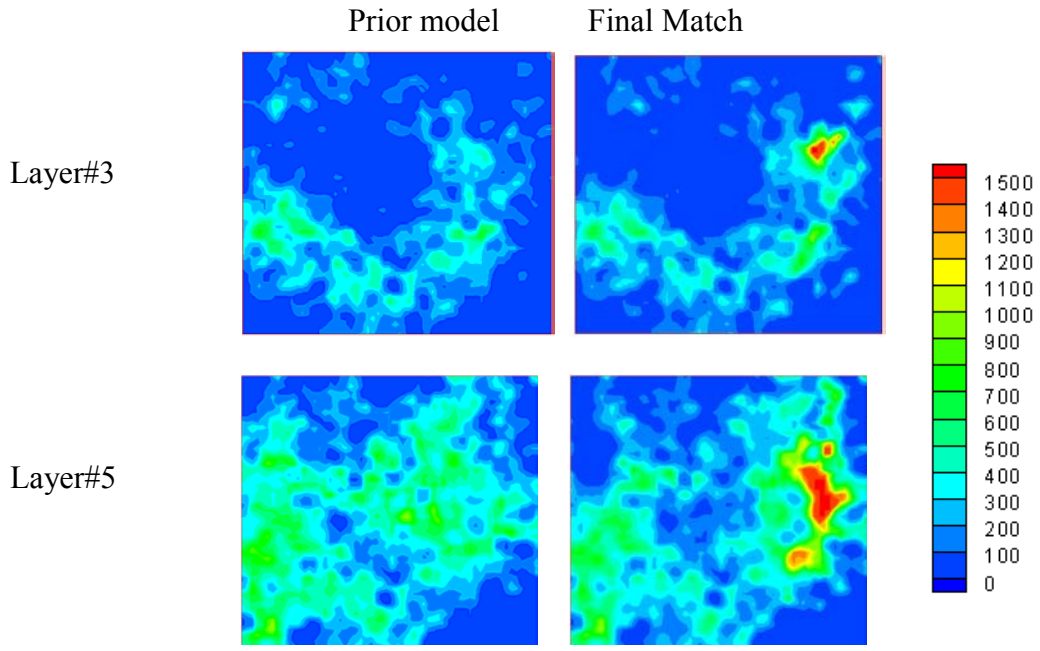

Fig. 23— Two layers illustrating changes to the prior model for matching production data. Note that much of the prior model remains unchanged to preserve geologic realism.

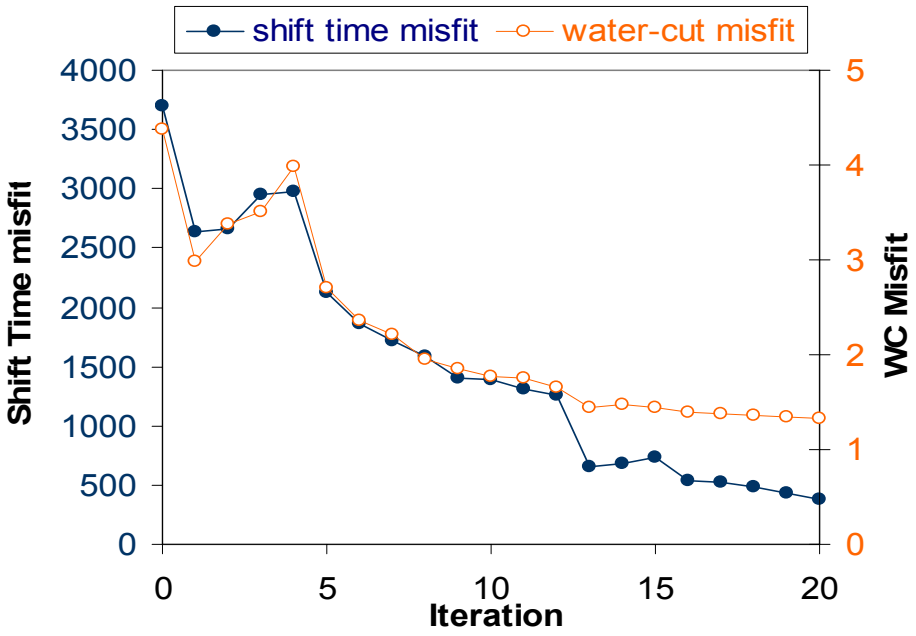

Fig. 24—Misfit vs. number of iterations (prior model-2)

CONCLUSIONS

Part-I

In this work we highlight the similarities between streamline-based assisted and automatic history matching. We enhance the streamline-based assisted history matching in two important aspects that can significantly improve its efficiency and effectiveness. First, we utilize streamline-derived analytic sensitivities to relate the changes in reservoir properties to the production response. These sensitivities can be computed analytically and contain much more information than that used in the assisted history matching. Second, we utilize the sensitivities in an optimization procedure to determine the spatial distribution and magnitude of the changes in reservoir parameters needed to improve the history-match. By intervening at each iteration during the optimization process, we can retain control over the history matching process as in assisted history matching. This allows us to accept, reject, or modify changes during the automatic history matching process. We have demonstrated the power and utility of our approach using two large field examples.

Some specific conclusions from this study can be summarized as follows:

- Use of streamline-derived sensitivities can significantly improve the efficiency of assisted history matching. In particular, the sensitivities can be utilized to directly obtain the changes in reservoir properties necessary to improve the history match in a more objective way. This eliminates the time-consuming and subjective manual adjustment of parameters in the assisted history matching process. By intervening at every stage of the iterative process, we can retain control over the history matching process to preserve plausibility and geologic realism.
- Streamline-based sensitivities and inversion allow us to take into account the full coupling of the streamlines in the reservoir rather than changing individual wells or streamline bundles at a time. This not only significantly increases the efficiency, but also preserves geologic continuity and minimizes the chances of introducing non-physical artifacts during the history matching process.
- The power and utility of streamline-based inversion is demonstrated using two field examples with model sizes ranging from 10^5 to 10^6 grid blocks and with over one hundred wells. In both the cases, the streamline-based automatic history matching led to better individual well matches as well as field-wide matches compared to assisted history matching and with no apparent loss of geologic realism. We have shown that the automatic history matching can be used both for conditioning geologic models and also to further improve the models derived from the assisted history matching.
- The use of sensitivities during assisted history matching can lead to significant savings in computation time and manpower. For the field examples presented here, the automatic history matching took days compared to months for assisted history matching. This makes it possible to generate multiple history-matched models to perform uncertainty analysis.

Part-II

We have proposed a streamline-based production data integration technique for naturally fractured reservoirs using the dual porosity approach. The principal features of our method are

the extension of streamline-derived analytic sensitivities to account for matrix-fracture interactions and the use of our previously proposed generalized travel time inversion for history matching. Our proposed workflow has been demonstrated by using both a dual porosity streamline simulator and a commercial finite difference simulator. The approach is computationally efficient and well suited for large scale field applications in naturally fractured reservoirs with changing field conditions. The use of the generalized travel time concept enabled us to match both the breakthrough and amplitude of the reference response in one step. The main findings of our study are summarized as follows.

- Streamline-based analytic sensitivity computations have been extended to naturally fractured reservoirs using the dual porosity approach. The matrix-fracture interactions are accounted for using predictor-corrector steps that involve convection along streamline followed by matrix-fracture exchange.
- A comparison of the streamline-based sensitivities with those computed using the numerical perturbation method shows close agreement, indicating the validity of our approach. The streamline-based sensitivity computation is extremely efficient and requires a single forward simulation.
- We have used the streamline-derived sensitivities in conjunction with a previously proposed generalized travel time inversion for integration of production data in fractured reservoirs. The generalized travel-time inversion is robust, computationally efficient and eliminates much of the time-consuming trial-and-error associated with manual history matching.
- We have combined the streamline-derived sensitivities with a dual porosity finite-difference simulator to exploit the efficiency of the streamline approach and the versatility of the finite-difference simulator. Use of finite-difference simulation allows us to include compressibility effects, strong matrix fracture coupling and cross-streamline mechanisms.
- We have demonstrated the power and efficiency of our proposed method using 2-D and 3-D examples designed after realistic field conditions. For the 3-D application, the results indicate the role of production data and prior information in terms of reproducing the fracture connectivity and fluid flow response in the reservoir.

REFERENCES

Part-I

1. Deutsch, C.V. and Journel, A.G.,1998. *GSLIB: Geostatistical Software Library and User's Guide*. 2nd edition, Oxford University Press, New York, 369pp.
2. Sun N.-Z., 1994. *Inverse Problem in Groundwater Modeling*. Kluwer Academic Publishers, Boston, 337pp.
3. Tarantola, H., 1987. *Inverse Problem Theory: Methods for Data Fitting and Model Parameter Estimation*. Elsevier, Amsterdam, Netherlands, 613pp.
4. Milliken, W.J. and Emanuel, A.: "History Matching Finite Difference Models with 3D Streamlines," paper SPE 49000 presented at the 1998 SPE Annual Technical Conference and Exhibition, New Orleans, 27-30 September.
5. Milliken, W.J., Emanuel, A. and Chakravarty, A.: "Application of 3D Streamline Simulation to Assist History Matching," paper SPE 63155 presented at the 2000 SPE Annual Technical Conference and Exhibition, Dallas, 1-4 October.
6. Baker R.O: "Streamline Technology: Reservoir History Matching and Forecasting = Its Success, Limitations, and Future," Distinguished Author Series, *Journal of Canadian Petroleum Technology*, April 2001, Vol.40, No. 4, 23-27.
7. Yeh, W. W.-G.: "Review of Parameter Identification Procedures in Groundwater Hydrology: The Inverse Problem," *Water Resources Research* (1986) **22**, No. 2, 95.
8. Wen, X.-H, Deutsch, C.V. and. Cullick, A.S.: "A review of Current Approaches to Integrate Flow Production Data in Geological Modeling," Report 10, Stanford Center for Reservoir Forecasting, Stanford, CA, 1997.
9. Cheng, H., Khargoria, A., He, Z. and Datta-Gupta, A.: "Fast History Matching of Finite-Difference Models Using Streamline-Derived Sensitivities," SPE 89447 presented at the SPE/DOE fourteenth symposium on Improved Oil Recovery, Tulsa, OK, April 17-21, 2004.
10. Landa, J.L. and Horne, R.N.: "A Procedure to Integrate Well Test Data, Reservoir Performance History and 4-D Seismic Information into a Reservoir Description," paper SPE 38653 presented at the 1997 SPE Annual Technical Conference and Exhibition, San Antonio, TX, Oct. 5-8.
11. Landa, J.L.: "Technique to Integrate Production and Static Data in a Self-Consistent Way," paper SPE 71597 presented at the 2001 SPE Annual Technical Conference and Exhibition, New Orleans, 30 September-3 October.
12. Wen, X.-H., Deutsch, C.V. and Cullick, A.S.: "High Resolution Reservoir Models Integrating Multiple-Well Production Data," *SPE Journal*, 344-355, December (1998).
13. Vasco, D.W., Yoon, S., and Datta-Gupta, A.: "Integrating Dynamic Data Into High-Resolution Reservoir Models Using Streamline-Based Analytic Sensitivity Coefficients," *SPE Journal*, 389, December (1999).
14. Wen, X.-H, Deutsch, C.V. and Cullick, A.S.: "Integrating Pressure and Fractional Flow Data in Reservoir Modeling With Fast Streamline-Based Inverse Method," paper SPE 48971 presented at the 1998 SPE Annual Technical Conference and Exhibition, New Orleans, 27-30 September.

15. Wang, Y. and Kovscek, A.R.: "Streamline Approach for History Matching Production Data," *SPE Journal*, 5, 353-363, 2001.
16. Caers, J., Krinshnan, S., Wang, Y. and Kovscek, A.R.: "A Geostatistical Approach to Streamline-Based History Matching," *SPE Journal*, 7(3), September (2002).
17. Agarwal, A. and Blunt, M.J.: "Streamline-Based Method with Full-Physics Forward Simulation for History-Matching Performance Data of a North Sea Field," *SPE Journal*, 8(2), June (2003).
18. Wen, X.-H., Deutsch, C.V. and Cullick, A.S.: "Inversion of Dynamic Production Data for Permeability: Fast Streamline-Based Computation of Sensitivity Coefficients of Fractional Flow Rate," *J. of Hydrology*, (2003), 281, 296-312.
19. Wu, Z. and Datta-Gupta, A.: "Rapid History Matching Using a Generalized Travel Time Inversion Method," *SPE Journal*, 7(2), 113-122, June (2002).
20. He, Z., Datta-Gupta, A., and Yoon, S.: "Streamline-Based Production Data Integration with Gravity and Changing Field Conditions," *SPE Journal*, 7(4), 423-436, December (2002).
21. Cheng, H., Datta-Gupta, A. *et al.*: "A Comparison of Travel-Time and Amplitude Matching for Production Data Integration Into Field-Scale Geologic Model," paper SPE 84570 presented at the SPE Annual Technical Conference and Exhibition, Denver, CO, October 5-8, 2003.
22. Agarwal, B., and Blunt, M. J.: "A Streamline-Based Method for Assisted History Matching Applied to an Arabian Gulf Field," paper SPE 84462 presented at the SPE Annual Technical Conference and Exhibition, Denver, CO, October 5-8, 2003.
23. Caers, J.: "Geostatistical History Matching Under Training-Image Based Geostatistical Model Constraints," *SPEJ* (2003), 218-226.
24. Liu, N., Betancourt, S., and Oliver, D.S.: "Assessment of Uncertainty Assessment Methods," paper SPE 71624 presented at the 2001 SPE Annual Technical Conference and Exhibition, New Orleans, 30 September-3 October.
25. King, M.J. and Datta-Gupta, A.: "Streamline Simulation: A Current Perspective," *In Situ* (1998) **22**, No. 1, 91.
26. Datta-Gupta, A., "Streamline Simulation: A Technology Update," SPE Distinguished Author Series, *Journal of Petroleum Technology*, 68-73 (December 2000).
27. Datta-Gupta, A. and King, M.J.: "A Semianalytic Approach to Tracer Flow Modeling in Heterogeneous Permeable Media," *Advances in Water Resources* (1995) **18**, No. 1, 9.
28. Datta-Gupta, A. *et al.*: "Streamlines, Ray Tracing and Production Tomography: Generalization to Compressible Flow," *Petroleum Geoscience* (May 2001), 75.
29. Bratvedt, F., Gimse, T. and. Tegnander, C.: "Streamline Computations for Porous Media Flow Including Gravity," *Transport in Porous Media*, 25(1), 63, 1996.
30. Vega, L., Rojas, D. and Datta-Gupta, A.: "Scalability of the Deterministic and Bayesian Approaches to Production Data Integration into Field-Scale Reservoir Models," SPE 79666 presented at the 2003 SPE Reservoir Simulation Symposium, Houston, 3-5 February.
31. Paige, C.C. and Saunders, M. A., 1982, LSQR: An algorithm for sparse linear equations and sparse least squares, *ACM trans. Math. Software*, 8(1), 43-71.
32. Durlofsky, L. J., Jones, R.C. and Milliken, W. J., "A New Method for the Scale Up of Displacement Processes in Heterogeneous Reservoirs," 4th Eurpoean Conference on Mathematics of Oil Recovery, Roros,Norway, June, (1994).

33. Schlumberger GeoQuest: FrontSim User Guide 2003A.

Part-II

1. Nelson, R. A. : Geological Analysis of Naturally Fractured Reservoirs, Gulf Publishing Company, Houston (1985).
2. Dershowitz, W., *et al.*: "Integration of Discrete Fracture network Methods with Conventional Simulator Approaches," *SPE Res. Eval. & Eng.*, 165-170, (April 2000).
3. Tamagawa, T., Matsuura, T., Anraku, T., Tezuka, K. and Namikawa, T., "Construction of Fracture Network Model Using Static and Dynamic Data," SPE 77741 presented at the SPE Annual Technical Conference and Exhibition, San Antonio, TX, Sept. 29-Oct. 2, 2002.
4. Long, J. C. S., Doughty C., Datta-Gupta, A., Hestir, K. and Vasco, D. W., "Component Characterization: An Approach to Fracture Hydrogeology," Subsurface Flow and Transport: The Stochastic Approach, G. Dagan and S. P. Neuman (Eds.), Cambridge University Press, 179-195 (1997).
5. Datta-Gupta, A., Vasco, D. W. and Long, J. C. S., "Detailed Characterization of a Fractured Limestone Formation Using Stochastic Inverse Approaches," *SPE Formation Evaluation*, 10 (3), 133-140 (1995).
6. Vasco, D.W., Yoon, S., and Datta-Gupta, A.: "Integrating Dynamic Data Into High-Resolution Reservoir Models Using Streamline-Based Analytic Sensitivity Coefficients," *SPE Journal* (1999), **4**(4), 389-399.
7. He, Z., Datta-Gupta, A., and Yoon, S.: "Streamline-Based Production Data Integration with Gravity and Changing Field Conditions*," SPE Journal*, 7(4), 423-436, December (2002).
8. Qassab, H, Khalifa, M, Pavlas, R., Khargoria, A., He, Z., Lee, S. H. and Datta-Gupta, A.: "Streamline-based Production Data Integration Under Realistic Field Conditions: Experience in a Giant Middle-Eastern Oil Reservoir," SPE 84079 presented at the SPE Annual Technical Conference and Exhibition, Denver, CO, October 5-8, 2003.
9. Wang, Y. and Kovscek, A.R.: "A Streamline Approach to History Matching Production Data," paper SPE 59370 presented at the 2000 SPE/DOE Symposium on Improved Oil Recovery, Tulsa, 3-5 April.
10. Milliken, W.J. *et al.*: "Application of 3-D Streamline Simulation to Assist History Matching," paper SPE 63155 presented at the 2000 SPE Annual Technical Conference and Exhibition, Dallas, 1-4 October.
11. Barenblatt, G.E., Zheltov, Iu. P., and Kochina, I.N.: "Basic Concepts in the Theory of seepage of homogenous Liquids in Fissured Rocks," j. Appl. Math. And Mech. Eng. Transl., 1286-1303, 1960.
12. Kazemi, H. et al.: "Numerical Simulation of Water-Oil Flow in Naturally Fractured Reservoirs," *SPEJ* (December 1976) 317-26: *Trans*., AIME 261.
13. Dean, R.H. and Lo, L.L.: "Simulations of Naturally Fractured Reservoirs," *SPERE* (May 1988) 638-48.
14. Di Donato, G., Huang, W., and Blunt, M.J.: " Streamline-Based Dual Porosity Simulation of Fractured Reservoirs," paper SPE 84036 presented at the 2003 Annual Technical Conference and Exhibition, Denver, CO, 5-8 October.
15. Al-Huthali, A.H.: "Streamline Simulation of Counter-current Imbibition in Naturally Fractured Reservoirs," Journal of Petroleum Science and Engineering, 2004 (in press).

16. Cheng, H, Khargoria, A., He, Z. and Datta-Gupta, A., "Fast History Matching of Finite-difference Models Using Streamline-derived Sensitivities," SPE 89447 presented at the SPE/DOE fourteenth symposium on Improved Oil Recovery, Tulsa, OK, April 17-21, 2004
17. Wu, Z. and Datta-Gupta, A.: "Rapid History Matching Using a Generalized Travel Time Inversion Method," *SPE Journal*, 7(2), 113-122, June (2002).
18. Cheng, H., Wen, X, Milliken, W. and Datta-Gupta, A., "Field Experiences with Assisted and Automatic History Matching Using Streamline Models," SPE 89857 presented at the SPE Annual Technical Conference and Exhibition, Houston, TX, September 26-29, 2004.
19. Oliver, D. S., Reynolds, A. C., Bi, Zhuoxin and Abacioglu, Y., "Integration of Production data Into Reservoir Models," Petroleum Geoscience, (7), S65-S73, 2001..
20. Guerreiro, L. *et al.*: "Integrated Reservoir Characterization of a Fractured Carbonate Reservoir." SPE 58995, SPE Inter. Petroleum Conf. and Exhib., Villahermosa, Mexico, (Feb. 2000).
21. King, M.J. and Datta-Gupta, A.: "Streamline Simulation: A Current Perspective," *In Situ* (1998) **22**, No.1, 91.
22. Datta-Gupta, A. and King, M.J: "A Semi-analytic Approach to Tracer Flow Modeling in Heterogeneous Permeable Media," *Advances in Water Resources* (1995) **18**, 9-24.
23. Pollock, D. W., "Semianalytical Computation of Pathlines for Finite-Difference Models," Groundwater, 26 (6), 743 (1988).
24. Kazemi, H. et al.: "Analytical and Numerical Solution of Oil Recovery From Fractured Reservoirs with Empirical Transfer Functions," *SPEJ* (May 1992) 219.
25. Bratvedt, F., Gimse, T. and Tegnander, C., "Streamline Computations for Porous Media Flow Including Gravity," Transport in Porous Media, 25, 63 (1996).
26. Bissel, R.C. *et al.*: "Reservoir History Matching Using the Method of Gradients," paper SPE 24265 presented at the 1992 SPE European Petroleum Computer Conference, Stavanger, 25-27 May.
27. Landa, J.L. and Horne, R.N.: "A Procedure to Integrate Well Test Data, Reservoir Performance History and 4-D Seismic Information into a Reservoir Description," paper SPE 38653 presented at the 1997 SPE Annual Technical Conference and Exhibition, San Antonio, TX, Oct. 5-8.
28. Wen, X. *et al.*: "High Resolution Reservoir Models Integrating Multiple-Well Production Data," paper SPE 38728 presented at the 1997 SPE Annual Technical Conference and Exhibition, San Antonio, Texas, 5-8 October.
29. Reynolds, A. C., He, N., and Oliver, D.S.: "Reducing Uncertainty in Geostatistical Description with Well Testing Pressure Data," in *Proc*., 1997 International Reservoir Characterization Conference, Houston, 2-4 March.
30. Anterion, F., Eymard, R. and Karcher, B. : "Use of Parameter Gradients for Reservoir History matching," paper SPE 18433 presented at the 1989 SPE Symposium on Reservoir Simulation, Houston, February 6-8.
31. Vega, L., Rojas, D. and Datta-Gupta, A.: "Scalability of the Deterministic and Bayesian Approaches to Production Data Integration into Field-Scale Reservoir Models," SPE 79666 presented at the 2003 SPE Reservoir Simulation Symposium, Houston, 3-5 February.
32. Paige, C.C. and Saunders, M. A.: "LSQR: An Algorithm for Sparse Linear Equations and Sparse Least Squares," *ACM Trans. Math. Software* (1982) **8**, No. 1, 43.
33. Vega, L., An Efficient Bayesian Formulation for Production Data Integration into Reservoir Models, Ph. D. Dissertation, Texas A&M University (December 2003).

34. Schlumberger GeoQuest: ECLIPSE User Guide 2003A.
35. Liu, N., Betancourt, S., and Oliver, D.S.: “Assessment of Uncertainty Assessment Methods,” paper SPE 71624 presented at the 2001 SPE Annual Technical Conference and Exhibition, New Orleans, 30 September-3 October.

LIST OF ACRONYMS AND ABBREVIATIONS

Part-I

$\boldsymbol{C_D}$ = data error covariance
$\boldsymbol{C_M}$ = prior model parameter covariance
f_w = fractional flow of water
$\boldsymbol{G}$ = sensitivity matrix
$\boldsymbol{I}$ = identity matrix
k = permeability
$\boldsymbol{L}$ = second spatial difference operator
m, $\boldsymbol{m}$ = reservoir parameter and its vector
$\boldsymbol{m_p}$ = prior reservoir model parameter
N_{dj} = number of dynamic data observations of jth well
N_w = number of wells
P = pressure
R^2 = coefficient of determination
s = slowness
S_w = water saturation
t = time
Δt = travel-time shift
$\Delta\tilde{t}$ = generalized travel time
$\boldsymbol{\Delta\tilde{t}}$ = generalized travel-time vector
y^{obs} = observed response
$\overline{y^{obs}}$ = averaged observed response
y^{cal} = calculated response
β_1 = weighting factor for the prior model
β_2 = weighting factor for the roughness term
λ_{rt} = total relative mobility
ϕ = porosity
τ = streamline time of flight

Part-II

D =Depth from datum, L
f = fractional flow, fraction
F_s = shape factor, L^{-2}
k = permeability, L^2
k_r = relative permeability, dimensionless
l = matrix length, L
P = pressure, $ML^{-1}T^{-2}$
P_c = capillary pressure, $ML^{-1}T^{-2}$
P_{gh} = pressure due to a gravity head in fracture system, $ML^{-1}T^{-2}$

q = source term, L^3T^{-1}
S = saturation, fraction
S_{orm} = matrix residual oil saturation, dimensionless
$S_{wn\ m}$ = normalized water saturation in matrix, dimensionless
t = time, T
u = velocity, LT^{-1}

Subscripts

f = fracture
i = grid-block or node index
m = matrix
n = time-step index
o = oil
w = water
x = x-direction
y = y-direction
z = z-direction